Zootaxa 4379 (3): 301–346
http://www.mapress.com/j/zt/

Article

ISSN 1175-5326 (print edition)
ZOOTAXA
ISSN 1175-5334 (online edition)

https://doi.org/10.11646/zootaxa.4379.3.1
http://zoobank.org/urn:lsid:zoobank.org:pub:8460642E-1216-4C69-B38D-33A2DC44353E

Taxonomic revision of Israeli snakes belonging to the *Platyceps rhodorachis* species complex (Reptilia: Squamata: Colubridae)

GUY SINAIKO[1,2,3], TALI MAGORY-COHEN[1], SHAI MEIRI[1,2] & ROI DOR[1,2]

[1]*School of Zoology, Tel-Aviv University, Tel-Aviv 6997801, Israel*
[2]*The Steinhardt Museum of Natural History, Tel-Aviv University, Tel-Aviv 6997801, Israel*
[3]*Corresponding author. E-mail: guysinaiko@gmail.com*

Abstract

The *Platyceps rhodorachis* species complex encompasses a widespread group of morphologically similar colubrid snakes. The number and identities of species from this complex in Israel have recently been debated. Studies from the previous decade concluded that there are two species in Israel and its vicinity (compared with one previously recognized), but their identity remained contested. We estimated the number of species and their taxonomic identity using morphological and molecular data. We found some evidence for clinal variation in many of the characters used to differentiate the species, and a great overlap in traits of putative species. Genetic data revealed very low sequence divergence, with all putative species being paraphyletic. *Platyceps rogersi* emerged as genetically closer to *Platyceps saharicus* rather than to its putative conspecific, *P. karelini*. The phylogenetic and taxonomic results thus indicate that the Israeli populations of the *P. rhodorachis* complex all belong to a single species, *Platyceps saharicus* (Schätti & McCarthy 2004).

Key words: *Platyceps saharicus*, Israel, Middle East, systematics, mtDNA, morphology

Introduction

The taxonomy of colubrid snakes of the genus *Platyceps* Blyth, 1860, has undergone many twists and turns. The genus *Platyceps* Blyth, 1860 was resurrected and split from *Coluber* Linnaeus, 1758 by Inger & Clark (1943). Inger & Clark (1943) based this segregation on dorsal scale row reductions, but this was not accepted by most authors (Nagy *et al*., 2004). The use of the generic name *Platyceps* began in the early 21st century, following molecular works that had found it to be monophyletic (Schätti & Utiger, 2001, Nagy *et al*., 2004). Today, the genus is thought to comprise 25 species (Uetz, 2017). The type species of *Platyceps* Blyth, 1860, *P. rhodorachis* (Jan 1865), was described from Iran. Its lectotype, MSNG 30312 (Kramer & Schnurrenberger, 1963), is from Shiraz, Iran (fide Schätti *et al*., 2014).

The *Platyceps rhodorachis* complex is a species complex comprised of morphologically similar taxa: *P. r. rhodorachis*, *P. r. ladacensis* Anderson, 1871, *P. r. subniger* Boettger, *P. rhodorachis* var. *tessellata* Werner, 1910, *P. saharicus* Schätti & McCarthy, 2004, and *P.* sp. *incertae sedis* (sensu Schätti & McCarthy, 2004). The species belonging to this complex are distributed from North Africa (south-eastern Algeria) and the horn of Africa, to southern Kazakhstan and north-western India (Sindaco *et al*., 2013). Snakes belonging to this complex are not found in Turkey, most of Iraq, northern and eastern Saudi Arabia (apart from the north-west regions) and eastern Jordan (Schätti *et al*., 2014, Sindaco *et al*., 2013). This geographic gap is thought to reflect a true absence of snakes belonging to this complex from those areas rather than being an artifact of insufficient collecting (Schätti *et al*., 2014). In the context of this geographic gap, *P. r. rhodorachis* and *P. r. ladacensis* can be referred to as eastern species in this complex, while the other aforementioned taxa can be referred to as western species (Fig. 1).

In Israel, snakes belonging to the *P. rhodorachis* species complex are known as “slender racers” (“zaamanim dakim” in Hebrew). They have two morphs, each with a distinct color pattern. The "banded” morph has a dorsal band between each pair of dark collars, and the lateral area of its head is gray (Fig. 2). The "non-banded” morph has dark dorsal collars with no light bands between them, and the lateral parts of its head are yellow (Fig. 2). Until

Accepted by Z. Nagy: 15 Dec. 2017; published: 15 Feb. 2018

the mid-20th century, only specimens of the non-banded morph had been found in Israel, all of them in desert areas. The first banded individual was found in 1953 near Jerusalem (HUJ 3652), in a Mediterranean climate biome (Werner, 1998). As more individuals of the banded morph were found, they were initially regraded as non-indigenous but, rather, as invasive individuals introduced by travelers. Eventually, however, it was concluded that they were indeed part of the local Israeli fauna (Werner, 1998).

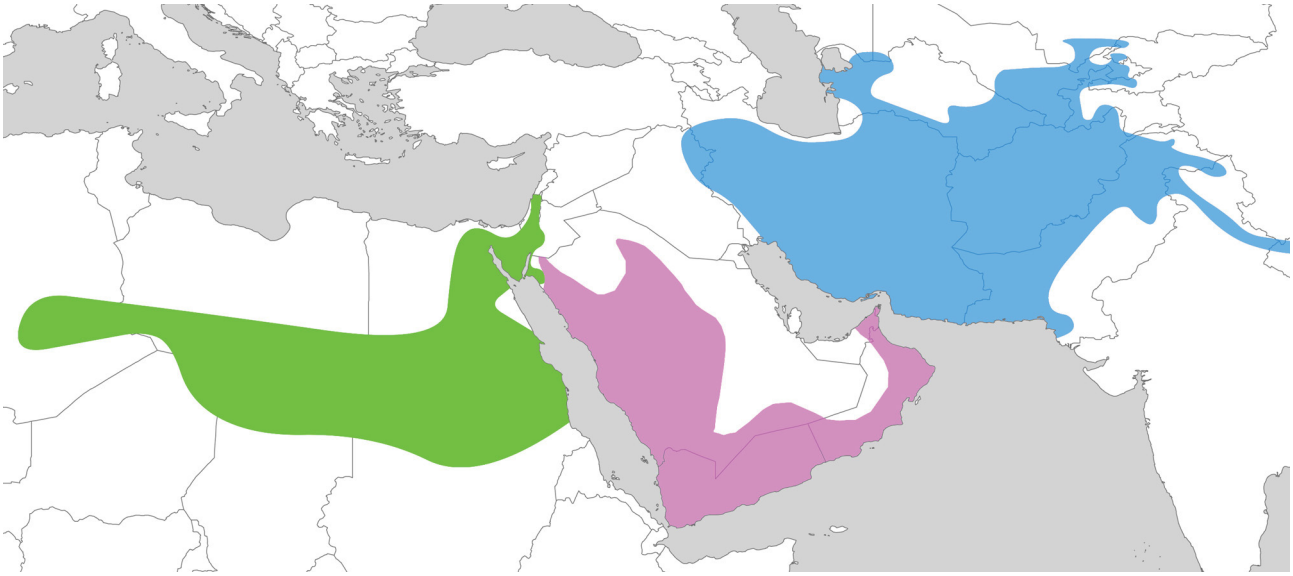

FIGURE 1. Distribution map of eastern and western taxa in the *P. rhodorachis* complex. Blue: eastern *P. rhodorachis* (adapted from Schätti *et al*., 2014). Purple: Arabian *P. rhodorachis* (adapted from Cox *et al*., 2006). Green: *P. saharicus* and *P.* sp. *incertae sedis* (adapted from Schätti & McCarthy, 2004, Geniez & Gauthier, 2008 and our own data).

FIGURE 2. Differences in dorsal color pattern of Israeli slender racers. Upper photos—banded morph with light bands between the dorsal collars. Lower photos—non-banded morph, with no light bands between the dorsal collars and with a yellow head. The bands of the banded morph are marked by arrows.

Banded and non-banded color morphs have been known from the Middle East since the 19th century, and individuals belonging to both morphs were assigned to four taxa. Tristram (1884) noted a related species, *Zamenis ventrimaculatus* Gray, 1834, from the Dead Sea area (now BMNH64.8.23.108). This species (now *Platyceps ventromaculatus*) is distinguished by a nuchal streak that is not present in snakes from the *P. rhodorachis* complex (Schätti *et al*., 2014). Tristram's specimen does not have such a nuchal streak, and in fact belongs to the banded morph of the *P. rhodorachis* complex (G.S., pers. obs.). This specimen, which was also mentioned by Günther (1865), was assigned by Schätti & McCarthy (2004) to "*Platyceps* sp. *incertae sedis*". Two specimens belonging to

the non-banded color morph (G.S., pers. obs.), collected by Richard Francis Burton from 'Midian' (northern Arabian Peninsula), were assigned by Günther (1878) to *Z. ventrimaculatus*. Those specimens, BMNH 77.6.1.7-8, were re-assigned by Schätti & McCarthy (2004) to a new species that they described: *Platyceps saharicus*.

Bodenheimer (1935, 1953) noted that *Coluber rhodorachis* was found in the Negev Desert of Israel. He contended that *C. ventromaculatus* was also to be found around the Dead Sea. Later authors, starting with Barash & Hoofien (1956), referred to only one species: *C. rhodorachis*. Arbel (1984) referred to the Israeli thin racers as *C. rhodorachis*, and noted that some large adult specimens featured a red dorsal stripe. Arbel (1984) contended that this stripe fades during preservation and can no longer be recognized in preserved specimens.

Werner (1988) recognized two subspecies in Israel, without naming them. He noted that one of them was to be found in the Mediterranean region and possibly also in the southern deserts, and that the other was to be found only in the southern deserts and in the southern Arava Valley. Werner (1995) contended later that the Israeli slender racers belong to two species that can be differentiated according to scale counts and color pattern. He considered the southern species, from the Arava and the Negev, to be of the non-banded morph, while the northern species, from the Jordan Valley and the Mediterranean area of Israel, to be of the banded morph. Bouskila & Amitai (2001) referred to the two morphs as belonging to a single species, *P. rhodorachis*, treating the morphs as mere geographic variants. They contended that the banded morph could only be found north of Ein Gedi (31.47N), and in the Mediterranean areas of Israel. Those authors also noted that a red dorsal stripe was only rarely present, and only in adult individuals.

Schätti & McCarthy (2004) reviewed the snakes belonging to the *P. rhodorachis* complex in Egypt and Israel, and assigned the Israeli slender racers to two species. The first species they described as *Platyceps saharicus* Schätti & McCarthy (2004; type locality: St. Catherine's Monastery area, Wadi el Sheikh, Egypt, holotype FMNH 72018). *Platyceps saharicus* was differentiated from *P. rhodorachis* in possessing more ventrals (238–264 vs. 221–237), in lacking the red dorsal stripe and in a ~1,000km geographic gap (Schätti & McCarthy, 2004). Schätti & McCarthy (2004) regarded the other species they considered to inhabit Israel as *Platyceps* sp. *incertae sedis*, and noted it was being reviewed by Gad Perry.

Platyceps rhodorachis is currently considered to be distributed in the vicinity of Iran and north-eastern Iraq, and *P. saharicus* in western Jordan, Israel, Egypt, Libya, south-eastern Algeria and eastern Chad (Schätti & McCarthy, 2004; Geniez, 2015). Geniez & Gauthier (2008) extended the distribution of *P. saharicus* to northern Chad and south-east Algeria. According to Schätti & McCarthy (2004), *Platyceps saharicus* and *P.* sp. *incertae sedis* further differ in ventral and subcaudal counts (ventrals: 238–264 in *P. saharicus*, 221–232 in *P.* sp. *incertae sedis*; subcaudals: 134–149 in *P. saharicus*, 124–133 in *P.* sp. *incertae sedis*). They also differentiate geographically, as *P.* sp. *incertae sedis* was not considered to inhabit Sinai and *P. saharicus* was not considered to inhabit northern Israel (Schätti & McCarthy, 2004). Schätti & McCarthy (2004) noted that no conclusive differences in coloration between the two species were known to them, and that further research was needed in this regard. Despite this, there is an overlap between *P. saharicus* and the non-banded morph, and between *P.* sp. *incertae sedis* and the banded morph (almost all individuals were classified by Schätti & McCarthy (2004) accordingly).

Schätti & McCarthy (2004) differentiated between *P.* sp. *incertae sedis*, and *P. rhodorachis* by the former always lacking a red dorsal stripe. They recognized it as similar to *rhodorachis* in head shield characteristics and in ventral count (221–232 in *P.* sp. *incertae sedis,* 221–237 in *P. rhodorachis*). They depicted *P.* sp. *incertae sedis* as distributed from the northern Palestinian Authority territory, to the central Negev and to south-western Jordan (Schätti & McCarthy, 2004).

Perry (2012) also referred to the Israeli slender racers as two distinct species, overlapping only slightly geographically. He referred to the banded morph as "northern Israeli", and to the non-banded morph as "southern Israeli". He differentiated the two species according to their color morph (banded versus non-banded) and ventral counts, which he found to be higher in the non-banded morph, although the ranges of ventral counts overlapped (209–245 in the northern species and 223–264 in the southern one). According to Perry (2012), the name *P. rhodorachis* could only apply to snakes featuring a red dorsal stripe, and as none of the Israeli specimens displayed this character, this taxon does not reside in Israel.

Perry (2012) identified the non-banded morph (*P. saharicus* according to Schätti & McCarthy, 2004) as *P. tessellata*, mainly due to the bright yellow head. A yellow head is mentioned in the description of *Zamenis rhodorachis* var. *tessellata* Werner, 1910. According to Perry (2012), *P. saharicus* could be a junior synonym of *P.*

tessellata, "based on range, appearance, and scale counts". Werner (1910) described *Z. r.* var. *tessellata* from "Asia Minor", (holotype IRSNB 2027). He noted that if the locality was correct, then it would be considered a new species in Asia Minor. Most authors refer to this locality as erroneous, and ignore this taxon altogether (Schätti *et al*., 2014), as no snakes of the *P. rhodorachis* complex have since been found in Turkey (Fig. 1).

Perry (2012) identified the banded morph (*P.* sp. *incertae sedis* in Schätti & McCarthy, 2004) as *P. ladacensis*, due to similarities in color pattern. He raised both *P. r*. var. *tessellata* and *P. r. ladacensis* to species level, because of the lack of geographical overlap and the intergradation between the two taxa in Israel.

Platyceps r. ladacensis was described by Anderson (1871) from Ladakh. Anderson (1895) later synonymized this taxon with *P. rhodorachis*, following Boulenger (1893). The holotype of this taxon is currently thought to be ZSI 7273 (Zoological Survey of India, Jabalpur, Madhya Pradesh, India), but the specimen cannot be located (Schätti *et al*., 2014).

According to Schätti *et al*. (2014), the nominotypical subspecies, *P. r. rhodorachis*, has a variable color pattern, which can be summed up as three main color morphs: The first is uniform gray with a thin red longitudinal stripe. It is found "from Ilam south to the Strait of Hormoz, and east through Turkmenistan and a good part of Afghanistan to north Pakistan". The second, patterned color morph, has a variable pattern of dots and bands on a gray background. It is found "from the Kurdish Region and the eastern Caspian coast to Kyrgyzstan, and from the Shatt al-Arab area to at least the border area between Uttarakhand (India) and westernmost Nepal". The third color morph of *P. r. rhodorachis* is plain gray, without a pattern, and is found in the Arabian Peninsula. The red-striped and the patterned color morphs are undistinguishable according to head shield characteristics; and the presence of a red stripe is not correlated with either age, sex, or altitude (Schätti *et al*., 2014). As far as we know, no molecular study has been performed regarding the status of those color morphs. According to Perry (2012), *P. rhodorachis* snakes that lack a red dorsal stripe, including those found in Iran, should be assigned to *P. ladacensis*. Most authors, however, recognize *P. rhodorachis* as having a variable color pattern and not always having a red dorsal stripe (Schätti *et al*., 2014; Geniez, 2015). Members of the two morphs have never been compared genetically.

Schätti *et al*. (2014) criticized Perry (2012) because the ventral counts of *P. ladacensis* and *P. tessellata* (sensu Perry) overlap. Furthermore, they considered that assigning an Israeli species to an Indian taxon (*P. ladacensis*), requires a "thorough reconsideration" of the geographical gap between the localities (Schätti *et al*., 2014).

Later Israeli authors concurred with Perry (2012). Bar & Haimovitch (2013) and Werner (2016) referred to *P. ladacensis* and *P. tessellata*, with the former authors naming *P. ladacensis* (the banded morph)—"zaaman yehuda" (Judean racer).

Perry (2012) noted that ventral counts could change along geographical gradients but he could not explore it further due to lack of data. Almost no molecular analyses compared species belonging to the *P. rhodorachis* complex, and none included Israeli specimens. Species delineation based on morphology alone can be misleading because of certain biases, such as convergence or plesiomorphy (Edwards *et al*., 2012; Sanders *et al*., 2013, Bryson *et al*., 2011).

We aim to clarify the taxonomic status of the slender racers of Israel and its vicinity, using morphological and molecular characters. We focused on the following questions:

How many slender racer species are there in this region?

Are there characters that allow classification of a specimen to two or more of the species; and if so, what are they?

To which species do slender racers in Israel belong?

Materials and methods

We examined the morphology of 207 specimens belonging to the *P. rhodorachis* complex: 132 of them from Israel and the Palestinian Authority, 25 from Egypt, 27 from Iran, 17 from Saudi Arabia, three from Iraq, one from Afghanistan, one from India, and one from Jordan (Appendix 1). We conducted molecular analysis of 49 of those specimens: 40 from Israel and the Palestinian Authority, two from Egypt, three from Saudi Arabia, two from Iran, one from Jordan, and one from Oman, as well as specimens from closely-related taxa as outgroups (Appendix 1., and see below). We documented 42 observations of slender racers from Israel and Jordan from the World Wide Web, most of them from a Facebook group dedicated to nature photography (www.facebook.com/groups/bugsphoto). We only documented observations presenting reliable data regarding the locality and date, and a

reasonable photograph of the individual (verified by G.S.) that allowed unambiguous classification of a snake to either the banded or non-banded morph. We used these data only to infer the geographic distribution of the two morphs and did not include them in any analyses. Acronyms of institutes housing the examined specimens are detailed in Appendix 1.

We followed Dowling's (1951) method for counting ventrals and subcaudals. G.S. conducted all measurements. We followed the terminology, and methods of measurement and reporting of Schätti *et al*. (2014). The only exceptions are that median/lateral (dorsal) locations of dorsal scale rows reductions (DSRDL) are given as the average number of the two uniting scale rows (e.g. if rows 4 and 5 are reduced to one row, then the median/lateral location is reported as 4.5); and the latitudinal location is reported separately for each half-reduction (e.g. 19–18, 18–17 etc.).

We measured total length (TOL), snout-vent length (SVL), and tail length (TL) of the specimens to the nearest 1.0 mm by copying the snake's midline to a slide through a squeezebox, scanning the slide, and measuring the line via Rhinoceros V5.5 software. The squeezebox method produces only 1% error whereas stretching produces 5%-10% error (McDiarmid *et al*., 2012).

We measured the following characters: head length and width (HL, HW), rostral height and width (RH, RW), loreal height and width (LH, LW), frontal length and width (FL, FW), internasal and prefrontal length (INP), parietal length (PL), the distance between the nostril and the eyeball (DNE), upper and lower chin shield length (CSU, CSL), and the eyeball diameter (ED). We measured all morphometric characters using a digital caliper to the nearest 0.1 mm, under a magnifying glass (x5).

We counted the following meristic characters: number of supralabials touching the eye (STE), temporal shields in the second temporal row (TEMP), supralabials (SUPLA), sublabials (SUBLA), preoculars (PREOC), postoculars (POSTOC), suboculars (SUBOCS), gulars (GUL), ventrals, subcaudals, total number of somites, dorsal scale rows reductions formula (DSRANT, DSRMID, DSRPOST), longitudinal (ventral) location of the dorsal scale rows reductions; expressed both as an exact ventral location (DSRVLex) and as a percentage of total ventral count (DSRVLpct), median/lateral (dorsal) location of the dorsal scale rows reductions (DSRDL), and the presence (or lack) of a fourth dorsal scale rows reduction (DSR4th). We measured the eyeball diameter at its maximal length (Razzetti *et al*., 2007). We recorded whether the anal plate was divided or not (AP).

Morphological analyses. We conducted all of the statistical analyses in R, version 3.3.1 (R Core Team, 2016). Bilateral characters can significantly differ between the left and right side of a specimen (Razzetti *et al*., 2007). We used a student's t-test to determine whether there were such differences in all continuous, bilateral characters (Appendix 2). We found a significant bilateral difference in five of the six characters, and conducted all further analyses separately for each side in those characters. We used the data from the right side for the rest of the bilateral morphometric characters, supplementing missing right side data with that from the left side in a few specimens. We analyzed all the categorical, bilateral characters separately for each side.

In accordance with the aforementioned geographical gap between the areas of distribution (Schätti *et al*., 2014) we refer to specimens from Israel and its vicinity as "the western sample". Specimens from Iran and eastwards, and specimens from the Arabian Peninsula, are referred to as "the eastern sample" (Fig. 1).

We examined histograms of all morphometric characters in the western sample (*P. saharicus* and *P.* sp. *incertae sedis,* or *P. tessellata* and *P. ladacensis* depending of the authors) for bimodal distributions, which could suggest that these specimens came from two separate populations. We assumed that if the western sample was composed of two species, they would correspond to the banded and non-banded morphs (Schätti & McCarthy, 2004; Perry, 2012). We thus examined whether the morphological characters were significantly affected by morph as well as by sex (Lindell *et al*., 1993; Schätti *et al*., 2014), latitude (Dowling, 1950) and body size. Body size is thought not to affect snake meristic characters, as those are probably determined during embryonic development and do not change during later ontogeny (Ewert, 1985). Because body size does affect a wide array of morphological attributes of species (e.g., Peters 1983, Calder 1984), and can vary geographically in snakes (Pincheira-Donoso & Meiri 2013), we nonetheless examined whether it can predict meristic traits such as scale counts. We used SVL as a proxy to body size, as it has an advantage over body mass within a species, which is more prone to change during an individual's life time, because of its reproductive and nutritional status and because of seasonality (Feldman & Meiri, 2013). We sexed the specimens using a probe, following Laszlo (1975).

Some of the data were not normally distributed (via Shapiro–Wilkes test) and some were heteroscedastic (examined via Levene's test). We therefore used exact permutations for our statistical analyses instead of parametric tests (Wheeler & Torchiano, 2016). We used a 10,000 steps bootstrap to assess confidence intervals.

We analyzed each continuous character separately, by conducting a linear model selection for each character, in turn, as the response variable. We tested the effects of four predictors (morph, sex, SVL and latitude), starting with a full model and following a backwards stepwise elimination procedure ($\alpha = 0.05$). This allowed us to assess the influence of the morphs on each character, in comparison to the other predictors. If the morphs were found to be the most prominent factor affecting other morphological characters, this could support the hypothesis that they represent two distinct species. Ventral and subcaudal counts had been argued to distinguish between species by previous authors (Schätti & McCarthy, 2004, Perry, 2012). To test whether latitude, SVL, and morph affect the variation in these counts we compared multiple predictor models using the Akaike Information Criterion (AIC). Following the suggestion by Arnold (2010), we consider models with $\Delta AIC < 2$ inferior to the models with lower AIC values that are nested in them, because in the more complex models model deviance is not penalized to an extent sufficient to overcome the 2-unit increase.

We analyzed each categorical character separately, conducting a Fisher's exact test in order to determine whether the frequency of each character condition was related to the color morphs.

In order to determine which characters, if any, could distinguish between the two morphs in the western sample, we observed whether the color morphs overlapped. We then checked whether it was possible to classify specimens to a morph via a machine learning tool. We conducted supervised machine learning using an artificial neural network model ("nnet" package in R) with k-fold cross-validation (k=5) (Olden *et al*., 2008) over 20 cycles. Morph was used as the response variable and morphological characters were used as predictors. This method allocates 20% of the data as "training data", upon which the machine creates rules that should allow it to classify according to a preliminary determination by a human. This is the "supervision" - which snake is banded and which is non-banded was decided in advance (by G.S.). In each cycle the machine chooses randomly a different set of 20% of the data as its training data, creates rules of classification, and seeks to implement these on the remaining 80%. In this way, none of the data are 'burned' as training data only. If the morphological characters allow the creation of classification rules that have a non-significant average error rate (<0.05), then it can be used as an argument in favor of more than one species in the dataset.

The machine learning method has advantages over parametric methods, as it enables modeling of non-linear associations in the dataset and requires no preliminary assumptions regarding the distribution of the independent variables (Olden *et al*., 2008).

We checked whether character states overlapped between the western sample as one unit, disregarding the color morphs, and the eastern sample. We also compared the characters of the type specimens of *P. r. rhodorachis*, *P. r. ladacensis*, *P. rhodorachis* var. *tessellata*, and *P. saharicus* from the literature (Schätti & McCarthy, 2004; Perry, 2012; Schätti *et al*., 2014) and from photographs, to the range of the western sample.

Molecular analyses. We analyzed 42 specimens belonging to the western sample, three specimens of the eastern sample, and 15 outgroup specimens (Appendix 1). We isolated genomic DNA from 100% ethanol-preserved muscle tissue samples using the DNeasy Blood & Tissue Kit (Qiagen, Valencia, CA, USA). We used *Platyceps karelini* (Brandt, 1838), *P. collaris* (Müller, 1878) and *P. rogersi* (Anderson, 1893) as close outgroups, and *Hemorrhois nummifer* (Reuss, 1834) and *Spalerosophis diadema* (Schlegel, 1837), both from genera closely related to *Platyceps* according to Pyron *et al*., 2013, as more distant outgroups.

We sequenced individuals for three mitochondrial gene fragments, 12S ribosomal RNA (*12S*), cytochrome c oxidase subunit I (*COI*), and cytochrome b (*cytb*). We amplified the gene fragments for both strands using published primers. The primers, their references, and PCR conditions are listed in Appendix 3. We sequenced the gene fragments via cycle sequencing using a BigDye terminator v1.1 kit (Applied Biosystems, Foster City, CA, USA) over an ABI 3500xl DNA Analyzer. We checked the chromatographs manually and edited them using GENEIOUS 9.1.6 (Biomatter Ltd). We translated the coding gene fragments (*COI* and *cytb*) into amino acids and ensured that no stop codons were present. Therefore we assumed the sequences to be functional. We aligned each gene fragment separately using Clustal Omega V.1.2.2 (Goujon *et al*., 2010; Sievers *et al*., 2011). We calculated the number of the variable and parsimony informative sites and uncorrected *p*-distances using MEGA V.7 (Tamura *et al*., 2011). All sequences generated for this study were deposited in GenBank (Accession numbers MF767305–MF767406, and MG566073, detailed in Appendix 1).

Phylogenetic analyses and hypothesis testing. We performed phylogenetic analyses for each gene fragment separately and for the complete dataset of *12S* and *cytb*. We used JModelTest V.2.1.10 (Darriba *et al*., 2012; Guindon & Gascuel, 2003) to select the best model of sequence evolution under the Bayesian information criterion (BIC). The software indicated that HKY+G for *cytb* and TIM2+G for *12S* were preferable.

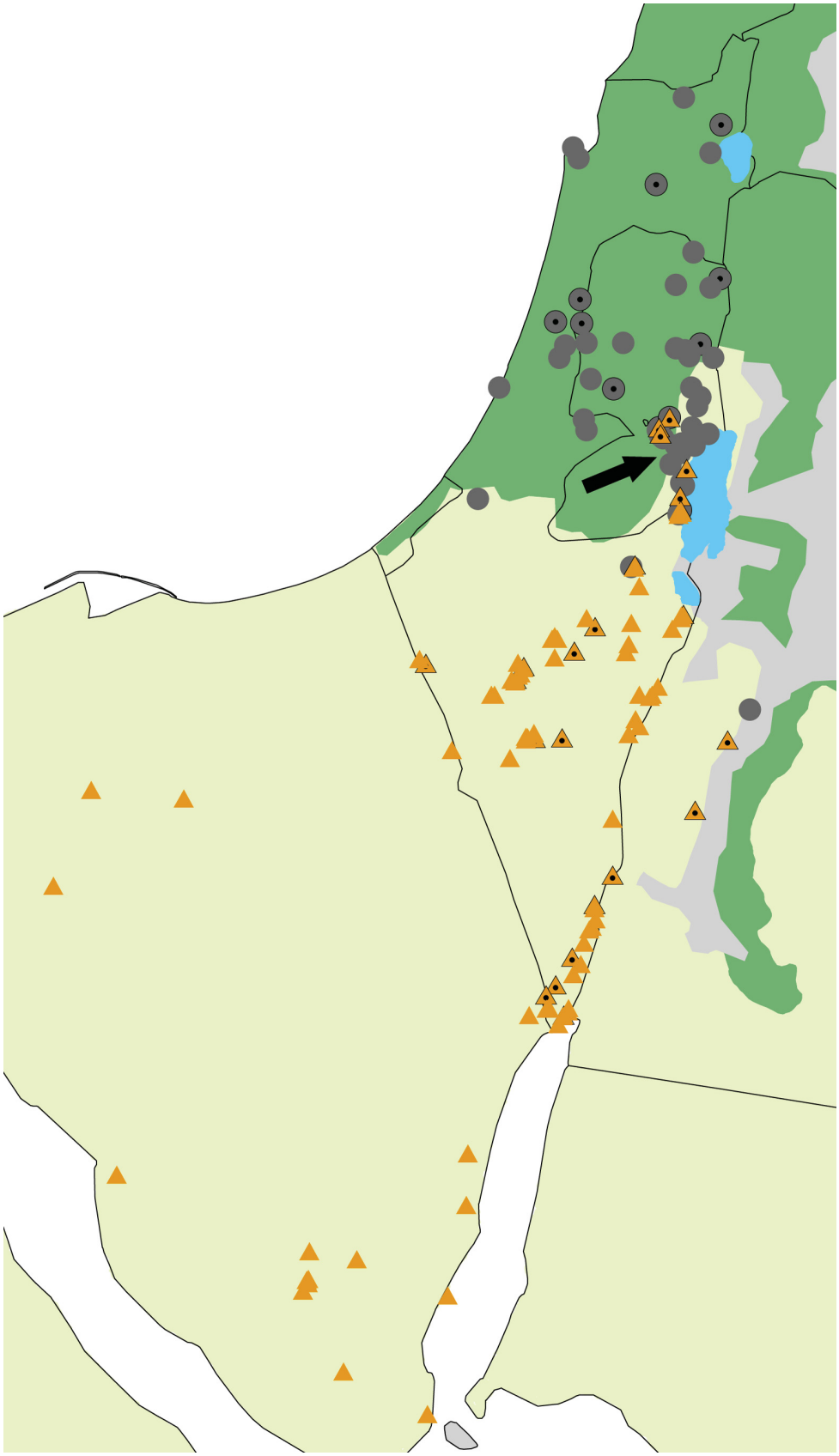

FIGURE 3. A map of the banded and the non-banded color morphs distribution along the desert and the Mediterranean biomes in Israel and its vicinity (biomes division according to Olson *et al*., 2001). The area of overlap between the two morphs is pointed at by an arrow. Gray circles: banded. Yellow triangles: non-banded. Black dot inside a symbol: observation only (no counts, measurements or genetic data). Green background: Mediterranean biome. Beige background: desert biome.

We performed phylogenetic analyses using maximum likelihood (ML) and Bayesian inference (BI) methods. We performed a ML analyses using RAxML v8.1.21 (Stamatakis, 2014) on raxmlGUI 1.5 beta (Silvestro & Michalak, 2012) with a general timereversible + Gamma distribution (GTR + G) model of evolution, parameters estimated independently for each partition. We assessed the reliability of the ML tree by bootstrap analysis comprising 1,000 replicants (Felsenstein, 1985). We considered nodes to be strongly supported if they received ML bootstrap values ≥ 80%.

We performed a BI analyses using MrBayes V.3.1.2 (Huelsenbeck & Ronquist, 2001, Ronquist & Huelsenbeck, 2003) with the closest model available in MrBayes being implemented to each gene partition and all parameters unlinked across partitions. We carried out two independent runs of 5 million generations and sampling frequency of every 1,000 generations. Convergence was assessed by examining stationarity in log-likelihood scores as the correlation of split frequencies between runs (AWTY; Nylander *et al*. 2008) and by examining effective sample size in TRACER v1.6 (Drummond & Rambaut, 2007). We discarded the first 25% of each run as burn-in, and the remainder was used to estimate tree parameters and topology. We then combined the remaining trees in a majority consensus tree. We assessed the reliability of the BI tree by calculating posterior probabilities (pp). We considered nodes to be strongly supported if they received pp values ≥ 0.9 (Huelsenbeck & Rannala, 2004).

Results

The distributions of both color morphs in Israel and its vicinity are shown in Fig. 3. The banded morph mostly inhabits higher latitudes and Mediterranean regions, while the non-banded morph mainly inhabits deserts at lower latitudes. The two morphs overlap in the Judean desert, a northwards extension of the desert biome in the rain shadow of the Judean Mountains to its west (Fig. 3).

Schätti & McCarthy (2004) classified NMW 25444.3-7, from Cairo, as *Platyceps* sp. *incertae sedis*, the equivalent to the banded morph in the current study. We examined photographs of these specimens and found that they actually belong to the non-banded morph, and therefore do not present any "geographic anomaly" by their presence in such a southern location as Cairo. Schätti & McCarthy (2004) classified the snakes according to their ventral counts and not by their color pattern, hence the peculiar labeling.

Morphological analyses. Three out of 42 continuous character values (dorsal locations of scales row reductions) show bimodal distributions (Fig. S1). All 42 continuous traits overlap between the two color morphs (Table 1).

Thirty-eight of the 46 continuous characters were significantly affected by at least one of the four predictors (morph: 12 characters, latitude: 25, SVL: 22 & sex: two) (Table 2). The ventral and subcaudal counts, previously considered to distinguish *P. saharicus* from *P.* sp. *incertae sedis* (Schätti & McCarthy, 2004) and *P. tessellata* from *P. ladacensis* (Perry 2012) overlap between the two morphs. Ventral counts range between 217–238 in the banded morph vs. 218–264 in the non-banded morph. Subcaudal counts range between 113–141 and 124–158 respectively. Ventral and subcaudal counts that were argued to distinguish *P. saharicus* from *P.* sp. *incertae sedis* (Schätti & McCarthy, 2004) or *P. ladacensis* from *P. tessellata* (Perry, 2012), show a latitudinal (clinal) pattern (Figs 5A, 5B).

The best model explaining variation in ventral counts is the one containing latitude alone ($R^2 = 0.709$; AIC = 733.6). Models with both morph or latitude ($R^2 = 0.706$, AIC = 735.5), or morph only ($R^2 = 0.377$, AIC = 928.1) are inferior (Arnold 2010). Subcaudal counts show similar results. The best model has latitude as a single predictor ($R^2 = 0.448$, AIC = 453.4) while models with morph and latitude ($R^2 = 0.440$, AIC = 455.5), or morph only ($R^2 = 0.210$, AIC = 548.4) are inferior. For both ventral and subcaudal counts, when using both morph and latitude as predictors, the effect of morph is not significant at $\alpha = 0.05$.

All 18 categorical character states overlap between the two color morphs. We found significant differences in frequencies of those character states between the two color morphs in four characters (Table 2). No variance was found in the following characters: anterior and middle scale row counts in the DSR formula (19 in all specimens), state of the anal plate (divided in all specimens), number of supralabials touching the eye (two in all specimens), and number of suboculars (one in all specimens). Therefore, these are not shown in Table 2.

TABLE 1. Comparison of means and ranges of all of the continuous characters, between the banded and the non-banded morphs in the western sample. Results originating from the left side of a specimen are marked by an asterisk.

Character	Banded				Non-banded			
	Range	Mean	SD	n	Range	Mean	SD	n
SVL	234–804	512.18	157.07	51	210–1043	591.82	193.92	96
TL	84–310	192.87	64.54	31	74–365	221.93	71.73	57
TOL	318–1114	660.10	215.68	31	284–1280	764.43	244.57	56
TL/SVL	0.36–0.45	0.41	0.02	31	0.27–0.46	0.41	0.03	56
VENTRALS	217–238	227.47	5.41	45	218–264	242.48	10.71	82
SUBCAUDALS	113–141	130.07	6.05	28	124–158	137.76	7.40	53
SOMITES	334–375	357.20	10.26	25	343–420	377.49	16.43	46
DSRVL1917ex	124–145.5	135.02	4.97	26	120–151.5	137.00	7.22	53
DSRVL1715ex	129.5–148	138.92	4.63	26	128.5–156	141.79	6.74	53
DSRVL1513ex	201–153.5	174.46	12.42	25	146.5–199	164.83	11.52	53
DSRVL1917pct	54.47–61.89	59.17	1.82	26	51.78–60.61	56.24	2.15	53
DSRVL1715pct	56.6–63.3	60.88	1.49	26	53.91–61.69	58.21	1.86	53
DSRVL1513pct	69.65–88.16	76.48	4.73	25	62.02–80.57	67.68	4.23	53
DSRDL1918	2.5–9.5	4.85	2.13	26	2.5–9.5	6.13	1.98	57
DSRDL1817	3.5–8.5	4.81	1.81	26	2.5–9.5	5.85	2.19	57
DSRDL1716	1.5–9.5	6.46	1.99	26	2.5–8.5	4.73	1.80	57
DSRDL1615	1.5–8.5	6.12	2.25	26	1.5–9.5	4.57	1.84	57
DSRDL1514	5.5–7.5	6.26	0.52	25	4.5–7.5	6.18	0.60	57
DSRDL1413	5.5–7.5	6.34	0.55	25	4.5–7.5	6.13	0.56	57
HL	9.4–19.9	14.23	2.82	49	9–20.7	14.09	2.85	99
HW	3.5–8.9	6.01	1.37	47	3.4–9.1	6.09	1.46	99
HL/HW	2.05–3.66	2.40	0.23	47	1.48–3.66	2.35	0.22	98
RW	1.6–4.1	2.86	0.70	48	1.3–4.9	2.93	0.78	97
RH	1.1–3.1	2.00	0.50	47	1.1–3.4	2.06	0.57	95
RW/RH	1.05–1.94	1.43	0.18	47	1.18–2	1.43	0.15	95
LW	0.6–1.8	1.32	0.33	43	0.4–2.4	1.42	0.42	96
LH	0.4–1.3	0.84	0.23	44	0.3–1.5	0.80	0.26	96
LW/LH	1.2–2.4	1.60	0.27	43	0.8–2.86	1.80	0.33	96
FL	3.2–6.4	4.88	0.86	49	3.1–7	4.88	0.86	100
FW	2–5	3.51	0.81	49	1.8–6.2	3.56	0.90	100
FL/FW	1.22–1.65	1.41	0.11	49	1.03–1.72	1.40	0.14	100
INP	2–5	3.43	0.83	48	1.4–6.1	3.55	1.03	99
FL/INP	1.21–1.76	1.44	0.14	48	0.97–2.21	1.43	0.21	99
PL	3.8–6.9	5.37	0.90	49	3.7–7.8	5.30	0.96	100
FL/PL	0.75–1.12	0.91	0.07	49	0.74–1.13	0.92	0.08	100
DNE	2.1–5	3.28	0.77	42	1.6–5.5	3.36	0.87	95
DNE*	1.8–4.5*	3.11*	0.73*	43*	1.5–5.2*	3.16*	0.83*	94*
DNE/INP	0.76–1.25	0.95	0.10	42	0.77–1.28	0.96	0.10	94
DNE/INP*	0.67–1.21*	0.90*	0.12*	43*	0.68–1.33*	0.91*	0.10*	93*
CSU	2.8–6.3	4.23	0.98	46	2.3–6.9	4.14	1.07	89

.....continued on the next page

TABLE 1. (Continued)

Character	Banded				Non-banded			
	Range	Mean	SD	n	Range	Mean	SD	n
CSU*	2.8–6.2*	4.15*	0.97*	43*	2.2–7*	4.10*	1.07*	90*
CSL	3.1–7.3	5	1.18	45	3–8.4	5.02	1.32	90
CSU/CSL	0.66–1.08	0.85	0.10	45	0.62–1.02	0.83	0.09	88
CSU/CSL*	0.69–1.06*	0.83*	0.09*	43*	0.6–1*	0.81*	0.09*	89*
ED	2.1–4	3.02	0.55	41	1.8–4.3	3.06	0.61	80
ED*	1.9–4*	3.01*	0.56*	39*	1.8–4.2*	3.01*	0.59*	80*

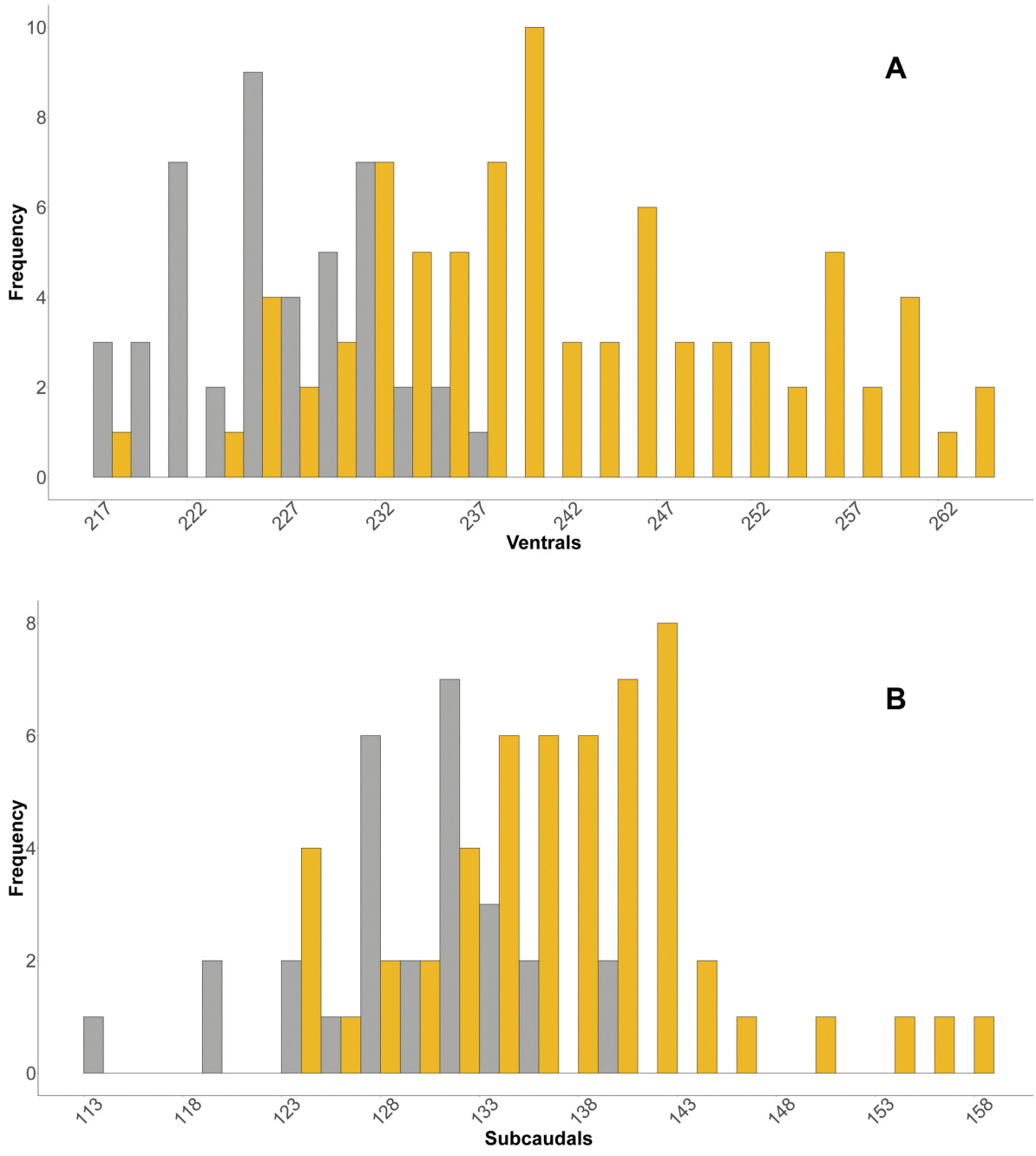

FIGURE 4. Histograms of ventral (A) and subcaudal (B) counts of the banded and the non-banded morphs in the western sample. Gray: banded morph. Yellow: non-banded morph.

TABLE 2. The minimum adequate models for the continuous characters. Results originating from measurements of the left side of a specimen are marked by an asterisk. R^2 values are given for the minimum adequate model of each character. Estimates shown are for non-banded versus banded morphs and for males versus females. SVL range from 210 to 1043 mm, the latitudinal range is 4.99 degrees. Number of specimens is given as (banded, non-banded). Range of each character values is given as minimum-maximum (range). Characters in which no variance was found are not presented.

Character	Morph		Sex		SVL		Latitude		R^2	Specimens	Range
	Estimate	P	Estimate	P	Estimate	P	Estimate	P			
SVL	NS	NS	NS	NS	NS	NS	NS	NS	NA	(51, 96)	210–1043 (833)
TL	NS	NS	NS	NS	0.4	<0.001	NS	NS	0.94	(31, 56)	74–365 (291)
TOL	NS	NS	NS	NS	1.4	<0.001	NS	NS	0.99	(31, 56)	284–1280 (996)
TL/SVL	NS	NS	NS	NS	NS	NS	NS	NS	NA	(31, 56)	0.27–0.46 (0.19)
VENTRALS	NS	NS	NS	NS	NS	NS	-8.84	<0.001	0.7	(42, 69)	217–264 (47)
SUBCAUDALS	NS	NS	NS	NS	NS	NS	-5.17	<0.001	0.45	(26, 46)	113–158 (45)
SOMITES	NS	NS	NS	NS	NS	NS	-13.51	<0.001	0.64	(23, 40)	334–420 (86)
DSRVL1917ex	NS	NS	NS	NS	NS	NS	-2.01	0.003	0.11	(24, 46)	120–151.5 (31.5)
DSRVL1715ex	NS	NS	NS	NS	NS	NS	-2.3	<0.001	0.18	(24, 46)	128.5–156 (27.5)
DSRVL1513ex	4.82	0.001	NS	NS	NS	NS	NS	NS	0.12	(24, 46)	146.5–201 (54.5)
DSRVL1917pct	1.04	0.003	NS	NS	NS	NS	0.6	0.033	0.39	(24, 46)	51.8–61.9 (10.1)
DSRVL1715pct	0.74	0.009	NS	NS	NS	NS	0.72	0.002	0.45	(24, 46)	53.9–63.3 (9.4)
DSRVL1513pct	2.81	<0.001	NS	NS	NS	NS	1.45	0.013	0.51	(24, 46)	62–88.2 (26.2)
DSRDL1918	-0.64	0.009	NS	NS	NS	NS	NS	NS	0.07	(26, 57)	2.5–9.5 (7)
DSRDL1817	-0.52	0.037	NS	NS	NS	NS	NS	NS	0.04	(26, 57)	2.5–9.5 (7)
DSRDL1716	0.87	<0.001	NS	NS	NS	NS	NS	NS	0.15	(26, 57)	1.5–9.5 (8)
DSRDL1514	NS	NS	NS	NS	NS	NS	NS	NS	NA	(25, 57)	4.5–7.5 (3)
DSRDL1615	0.77	0.001	NS	NS	NS	NS	NS	NS	0.11	(26, 57)	1.5–9.5 (8)
DSRDL1413	NS	NS	-0.14	0.03	NS	NS	NS	NS	0.06	(21, 43)	4.5–7.5 (3)
HL	NS	NS	NS	NS	0.015	<0.001	0.64	<0.001	0.86	(44, 81)	9–20.7 (11.7)
HW	NS	NS	NS	NS	0.007	<0.001	0.21	<0.001	0.82	(42, 81)	3.4–9.1 (5.7)
HL/HW	NS	NS	NS	NS	0	0	NS	NS	0.11	(45, 95)	1.48–3.66 (2.18)
RW	NS	NS	NS	NS	0.004	<0.001	0.12	<0.001	0.76	(43, 79)	1.3–4.9 (3.6)

……continued on the next page

TABLE 2. (Continued)

Character	Morph		Sex		SVL		Latitude		R^2	Specimens	Range
	Estimate	P	Estimate	P	Estimate	P	Estimate	P			
RH	NS	NS	NS	NS	0.003	<0.001	0.1	<0.001	0.76	(42, 77)	1.1–3.4 (2.3)
RW/RH	NS	NS	NS	NS	NS	NS	NS	NS	NA	(47, 95)	1.18–2 (0.82)
LW	-0.06	0.019	NS	NS	0.002	<0.001	0.09	<0.001	0.78	(39, 78)	0.4–2.4 (2)
LH	NS	NS	NS	NS	0.001	<0.001	0.06	<0.001	0.7	(40, 78)	0.3–1.5 (1.2)
LW/LH	-0.1	<0.001	NS	NS	NS	NS	NS	NS	0.07	(44, 81)	0.8–2.9 (2.1)
FL	0.09	0.033	NS	NS	0.004	<0.001	0.09	0.02	0.85	(44, 81)	3.1–7 (3.9)
FW	NS	NS	NS	NS	0.004	<0.001	0.15	<0.001	0.85	(44, 81)	1.8–6.2 (4.4)
FL/FW	NS	NS	NS	NS	0	<0.001	NS	NS	0.48	(47, 96)	1.03–1.72 (0.69)
INP	NS	NS	NS	NS	0.005	<0.001	0.19	<0.001	0.88	(43, 80)	1.4–6.1 (4.7)
FL/INP	NS	NS	NS	NS	-0.001	<0.001	-0.04	<0.001	0.5	(43, 80)	0.97–2.21 (1.25)
PL	NS	NS	NS	NS	0.005	<0.001	0.23	<0.001	0.81	(44, 81)	3.7–7.8 (4.1)
FL/PL	NS	NS	NS	NS	NS	NS	NS	NS	NA	(49, 100)	0.74–1.13 (0.39)
DNE*	NS*	NS*	NS*	NS*	0.004*	<0.001*	0.13*	<0.001*	0.86*	(40, 78)*	1.5–5.2 (3.7)*
DNE	NS	NS	NS	NS	0.004	<0.001	0.14	<0.001	0.89	(39, 78)	1.6–5.5 (3.9)
DNE/INP*	NS*	NS*	NS*	NS*	NS*	NS*	NS*	NS*	NA*	(43, 93)*	0.68–1.33 (0.65)*
DNE/INP	NS	NS	NS	NS	NS	NS	NS	NS	NA	(42, 94)	0.77–1.28 (0.51)
CSU*	NS*	NS*	NS*	NS*	0.005*	<0.001*	0.21*	<0.001*	0.86*	(40, 76)*	2.2–7 (4.8)*
CSU	NS	NS	NS	NS	0.005	<0.001	0.24	<0.001	0.86	(42, 75)	2.3–6.9 (4.6)
CSL	NS	NS	NS	NS	0.007	<0.001	0.23	<0.001	0.87	(41, 76)	3–8.4 (5.4)
CSU/CSL*	NS*	NS*	-0.02*	0.03*	NS*	NS*	NS*	NS*	0.04*	(28, 61)*	0.6–1.06 (0.47)*
CSU/CSL	NS	NS	NS	NS	NS	NS	NS	NS	NA	(45, 88)	0.62–1.02 (0.4)
ED*	NS*	NS*	NS*	NS*	0.003*	<0.001*	0.10*	<0.001*	0.82*	(36, 69)*	1.8–4.2 (2.4)*
ED	0.11	<0.001	NS	NS	0.003	<0.001	NS	NS	0.87	(41, 77)	1.8–4.3 (2.5)

TABLE 3. Frequency comparisons of categorical character states between the banded and the non-banded morphs in the western sample. P-values are for Fisher's exact tests. Results originating from the left side of a specimen are marked by an asterisk.

Character	P	States	Banded	Non-banded
DSRPOST	0.002	11 DSR	2	24
		13 DSR	36	67
		15 DSR	8	1
DSR4th	0.002	No	44	68
		Yes	2	24
TEMP	0.608	2	41	81
		3	5	14
TEMP*	0.053*	1*	3*	0*
		2*	32*	73*
		3*	10*	21*
SUPLA	0.271	8	0	1
		9	37	89
		10	4	3
SUPLA*	0.037*	9*	35*	86*
		10*	7*	4*
SUBLA	0.842	9	2	3
		10	34	72
		11	0	2
SUBLA*	0.007*	9*	4*	0*
		10*	30*	78*
		11*	0*	1*
PREOC	0.802	1	35	79
		2	7	14
PREOC*	1*	1*	37*	81*
		2*	5*	12*
POSTOC	0.1	1	2	0
		2	42	94
GUL	0.159	3	8	28
		4	29	63
		5	3	2
GUL*	0.83*	3*	6*	19*
		4*	32*	67*
		5*	2*	5*

We found that significant classification of a specimen into one of the color morphs, with an error rate ≤5%, was not possible. The average error of an artificial neural network based on all of the morphological characters was 54% (range: 29%–65%, std. dev. 11%). Using all of the characters reduced the sample size to 12 banded and 22 non-banded specimens. To increase the sample size we carried out a second analysis, using only SVL and the traits significantly associated with morph (Tables 2&3). In this analysis (based on 22 banded and 45 non-banded specimens), the mean error rate was 49% (range 23%–64%, std. dev. 11%), which does not significantly differ from a random error rate. In the second analysis most errors involved banded specimens that were wrongly classified as non-banded. Incorrectly classifying non-banded specimens as banded was less common—but 10 out of 45 non-banded specimens (22%) were nonetheless incorrectly classified as banded.

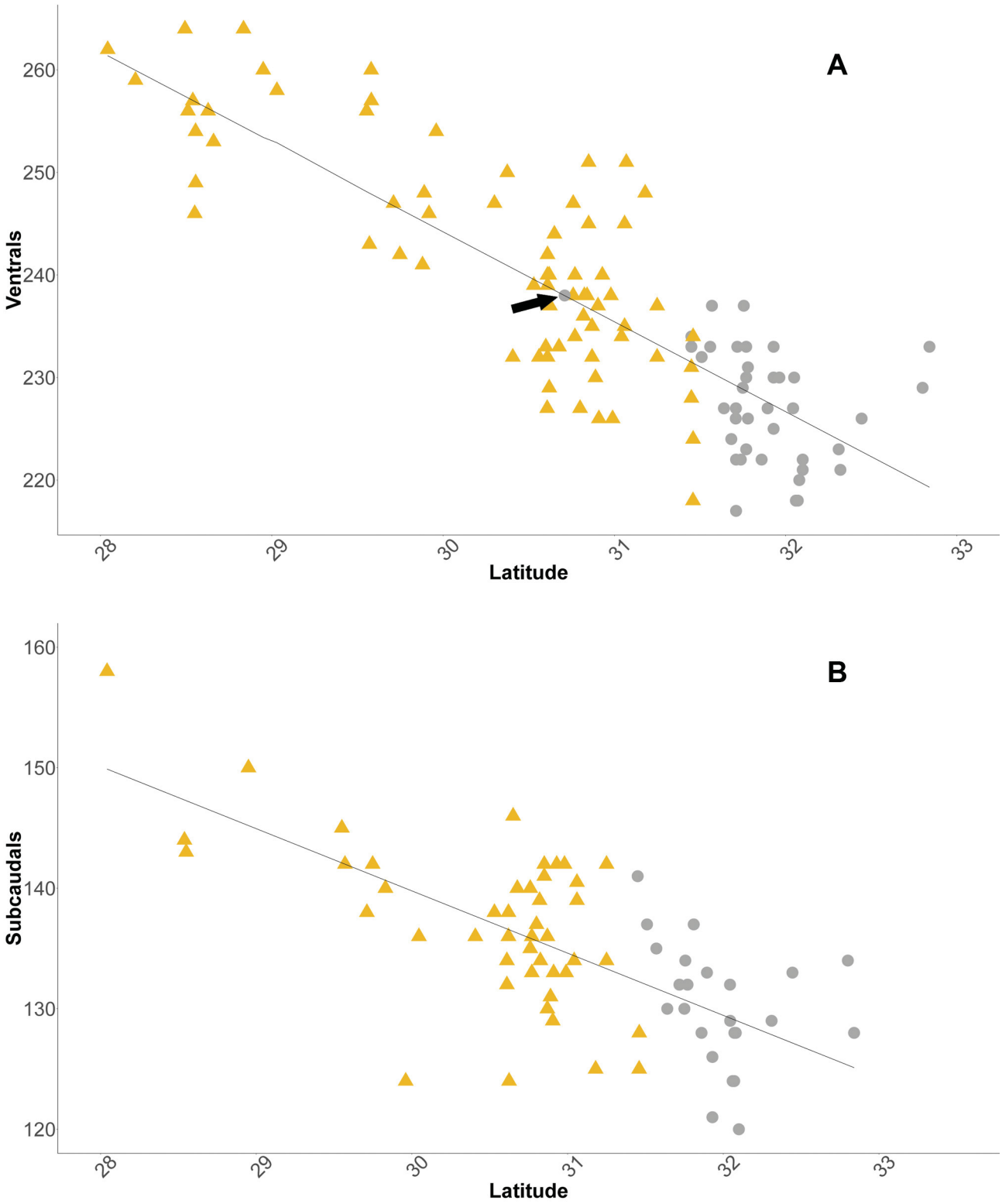

FIGURE 5. A) a regression of ventral counts versus latitude. HUJ21937 (a banded specimen from a distinctly low latitude—see discussion) is pointed at by an arrow. B) a regression of subcaudal counts versus latitude. Gray: banded morph. Yellow: non-banded morph.

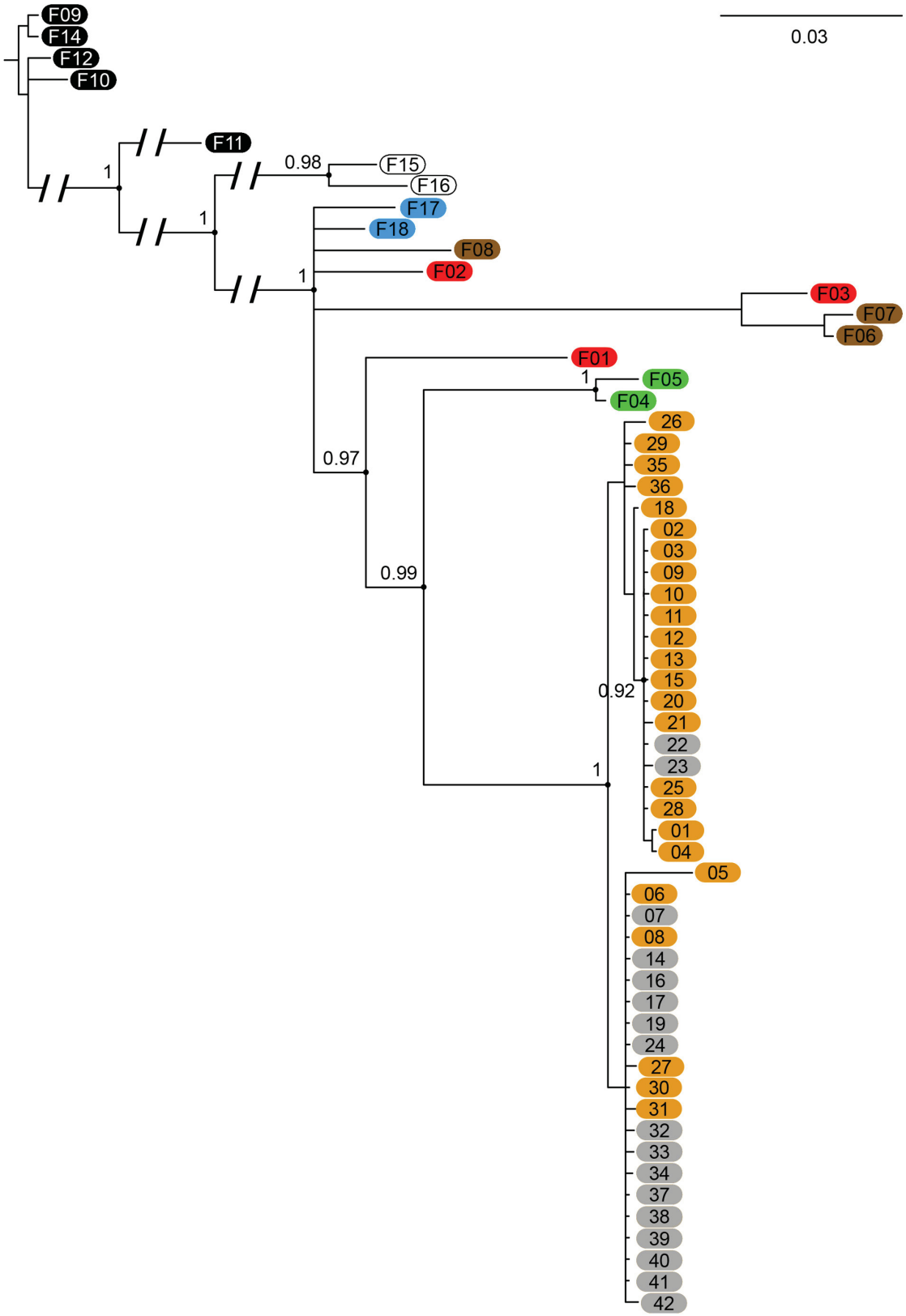

FIGURE 6. Consensus tree based on concatenated *cytb* and *12S* gene fragments. Support values are posterior probabilities of a Bayesian inference analysis. Samples 35 & 36 are from an area adjacent to the type locality of *P. saharicus* (Saint Catherine's Monastery in Sinai, Egypt). Values lower than 0.9 are not shown. Branches which are not shown to full length are indicated by / /. Gray: banded morph (western sample). Yellow: non-banded morph (western sample). Red: *P. rhodorachis* (eastern sample). Green: *P. rogersi*. Blue: *P. karelini*. Brown: *P. collaris*. White: *Hemorrhois nummifer*. Black: *Spalerosophis diadema*.

All 42 continuous character values overlap between the eastern and western samples (Appendix 4). Likewise, all 18 categorical character states overlap between the eastern and western samples. We found significant differences in frequencies of categorical character states between the two samples in six out of 18 characters (Appendix 5). A red dorsal stripe was not found in any of the western sample specimens. The characters that were uniform among the western sample were identical in the eastern sample.

The available character states of the type specimens of *P. r. rhodorachis*, *P. r. ladacensis, P. rhodorachis* var. *tessellata*, and *P. saharicus* fit within the range of at least one of the color morphs in the western sample (Appendix 6), except for the following: the holotype of *P. tessellata* has 12 DSR in the posterior location of the DSR formula, whereas snakes from the western sample have either 11, 13 or 15 DSR. The rostral width-height ratio in the holotype of *P. ladacensis* is lower than that of all the snakes in the western sample. Consequently, the morphology of the type specimens is unlikely to rule out the identification of western sample snakes with any of the aforementioned taxa—except perhaps *P. r. ladacensis* and *P. r.* var. *tessellata*.

Molecular analyses. We found very low variation in the nucleotide sequence of the *COI* gene fragment (548 bp; three haplotypes that differed in one bp, accession numbers are detailed in Appendix 1) across the 18 specimens we analyzed (6 banded and 12 non-banded, all from Israel and its vicinity), which was uninformative. Therefore, we did not sequence this gene fragment for additional specimens. The *cytb* gene fragment was 597 bp long. Twenty-three sites were variable and six were parsimony-informative. The *12S* gene fragment was 579 bp long, with 14 variable sites and four parsimony-informative ones. The genetic distances among all specimens of the western sample were smaller than those between the western sample and all other species in the genus *Platyceps*, including eastern representatives of the *P. rhodorachis* complex (Table 4).

TABLE 4. Sequence divergence values between taxa (given in percents). B: banded. NB: non-banded morph. Western: B. and N.B. non-segregated.

Divergence compared between taxa		12S	cytb
Western	Divergence between B. & N.B.	0.4	0.6
	Among B.	0.2	0.2
	Among N.B.	0.3	0.4
	Among western	0.3	0.5
Western & *P. rhodorachis*	Between B. & *P. rhodorachis*	5.7	12.0
	Between N.B. & *P. rhodorachis*	5.9	12.0
	Between western & *P. rhodorachis*	5.8	12.0
Western & *P. rogersi*	Between B. & *P. rogersi*	3.4	6.8
	Between N.B. & *P. rogersi*	3.1	6.6
	Between western & *P. rogersi*	3.2	6.7
Western & *P. karelini*	Between B. & *P. karelini*	5.2	11.7
	Between N.B. & *P. karelini*	5.4	11.6
	Between western & *P. karelini*	5.3	11.6
Western & *P. collaris*	Between B. & *P. collaris*	7.5	13.4
	Between N.B. & *P. collaris*	7.6	13.6
	Between western & *P. collaris*	7.5	13.5

The combined Bayesian inference phylogenetic tree based on concatenated *cytb* and *12S* gene fragments is presented in Fig. 6. The banded and non-banded specimens of the western sample together form a clade that is not further divided into two separate ones. Neither banded nor non-banded snakes form a clade. The sister group of the western sample is *P. rogersi*, and the next closest taxon to both *P. rogersi* and to the western sample is a *P. rhodorachis* from Oman (CAS 251164). The three *P. rhodorachis* specimens do not form a monophyletic group. Maximum likelihood tree and trees for the two gene fragments separately (Fig S2) show similar topologies.

Discussion

We found no evidence in either the molecular or the morphological data to support the recognition of two species from the *Platyceps rhodorachis* complex in Israel. We found little evidence for bi-modality. There was strong clinal variation in the most prominent character used to differentiate snakes into species (i.e. the number of ventrals). No trait enabled the classification of snakes to different morphs. Furthermore, genetic distances were very low across the western sample, and both morphs turned out to be paraphyletic, with little genetic structure in the population overall.

While we did detect some differences between morphs, we interpret most of the significant differences as being irrelevant. For example, the significant difference in the loreal width between the morphs (Table 2), is 0.06 mm, but the measurement precision for this character is 0.1 mm. Another example is the dorsal location of the dorsal scale rows reduction from 18 to 17 rows (Table 2). Despite the statistically significant difference, the model explains only 4% of the variance in this character. The biological significance of this difference between the morphs is likely to be negligible.

At least one diagnostic morphological character is required in order to differentiate the populations into two species (Helbig *et al*., 2002). Such determination may reflect a continuous character that has no overlap in values between the two populations or a categorical character that has a different state in each of them, thus indicating that there is no gene flow between them (Helbig *et al*., 2002). Even among subspecies there is a demand for a diagnostic character, the lack of which may be a strong argument against the validity of their subspecific rank (Manier, 2004). A more permissive approach allows the recognition of a species boundary if the diagnostic character is polymorphic, as long as the shared character state between the species occurs at a very low frequency (Wiens & Servedio, 2000). We found no character state that meets any of these conditions among the western sample specimens (Tables 1 & 3). As only three characters show a bimodal distribution (and these are probably non-informative, see below), even the phenetic clusters approach that allows for overlaps as long as the species are not assimilated into each other (Mallet, 1995), would not recognize more than one species in the western sample. The failure of the artificial neural network analysis in classifying a specimen to each of the color morphs with an error rate of less than 5% strengthens this result.

The color morphs themselves (the presence or lack of bands) is the only character that may allow us to segregate western sample specimens into two distinct groups. As the null hypothesis is the existence of a single species (Mallet, 1995), we reject the more complicated hypothesis (of having more than one species) as there is no morphological evidence to support it.

We found a strong latitudinal cline in ventral and subcaudal counts (Figures 5A & 5B). Such a pattern is commonly interpreted as a trait of a single species (Mayr, 1942), as none of the entities of the cline present an independent evolutionary trajectory that differs from that of the others (Kelly *et al*., 2008).

Osgood (1978) found that the number of ventrals in snakes may be affected by the temperature of the soil in which the eggs are laid. Such a correlation between ventral count and temperature can further strengthen our interpretation, regarding the lack of a phylogenetic signal in this character, rendering it a weak indicator for taxonomic purposes. The latitudinal cline better explains the variance in ventral and subcaudal counts than dichotomous division into morphs that Schätti & McCarthy (2004) and Perry (2012) suggested as the character best showing a species boundary.

The phylogenetic trees (Figs 6 & S2) do not indicate that the western sample comprises more than one species. The trees lack structure and do not show a division into two groups in accordance with color morph. Individuals of both morphs and with different ventral counts are found throughout the ingroup. The phylogenetic groups do not fit geographic mapping (Fig. S3) and both contain individuals from across the geographic range of the western sample. Individuals from adjacent areas are scattered in both groups.

Furthermore, sequence divergence among individuals of the western sample is low. The average *cytb* sequence divergence value in reptiles is 13.6% among congeneric species (Harris, 2002). The *cytb* sequence divergence value among individuals of the western sample is 0.5% (Table 4), which resembles the values found between conspecifics in other species [e.g., 1.6% among 37 individuals of *Hemorrhois hippocrepis* (Linnaeus 1758); Carranza *et al*., 2006]. The fact that the *COI* gene fragment is nearly identical among individuals of the western sample further strengthens this view.

The taxonomic identity of the western sample

Because of the four name-bearing specimens falls within the range of the morphological values of the western sample (Appendix 6), we cannot confidently rule out any of these four taxa as a possible identity for the western sample on this basis.

The ranges of all morphological characters overlap between the western and eastern sample (the latter comprising *P. rhodorachis* individuals and one *P. r. ladacensis*). The only character that differentiates them morphologically is the constant lack of the red dorsal striped color morph from the western sample—a feature that was not found in any of our western sample specimens. We were not able to find any actual observations that suggest the presence of a red dorsal stripe in a "slender racer" from Israel and its vicinity, either in preserved snakes or in live ones that we and others (Amos Bouskila, Aviad Bar, Boaz Shacham, Erez Maza, Simon Jamison, Philippe Geniez, pers. comm.) have examined, or in photographs from the internet. We further deduce that the western sample does not belong to *P. rhodorachis*, based on the molecular analysis. The phylogenetic tree suggests that the sister taxon to the western sample is *P. rogersi*, while *P. rhodorachis* is the sister taxon of a clade containing both the western sample and *P. rogersi* (Fig. 6). The sequence divergence between western sample snakes and eastern *P. rhodorachis* is 12%, compared to only 0.5% among the western sample individuals (Table 4). This 12% divergence value is similar to the divergence between *P. rhodorachis* and *P. rogersi* (11.1%), *P. collaris* (13.5%) and *P. karelini* (13.7%) (Appendix 7). The geographic gap between the eastern and western samples suggests that the genetic distance between *P. rhodorachis* and the western sample is not an artifact of isolation by geographic distance (Kelly *et al*., 2008). Therefore, a genetic cline between the populations of the western and the eastern samples is improbable.

We examined the holotype of *P. rhodorachis* var. *tessellat*a (IRSNB 2027) only from photographs. Its color pattern is somewhat similar to both the patterned color morph of *P. rhodorachis* and to that of the non-banded morph of the western sample. The collection data of the holotype, "Asia Minor", is probably erroneous (Schätti *et al*., 2014). We cannot unequivocally classify the holotype of *P. tessellata* to either the eastern or the western sample. We suggest that further research is necessary to shed light on this taxon; e.g., whether it is possible to analyze its stomach contents and try to infer its true collection locality (Mendelson *et al*., 2016). We found no evidence to suggest that *P. tessellata* is conspecific with the Israeli snakes (as suggested by Perry, 2012).

The assignment of the banded morph of the western sample to *P. ladacensis* is, in our view, improbable. The description by Anderson (1871) does not allow a distinction between *P. r. ladacensis* and the western sample, except for the rostral width-height ratio ("rostral as broad as high" in the description versus a ratio that exceeds that in the western sample snakes).

Our study included only one specimen assigned by Schätti *et al*. (2014) to *P. r. ladacensis* (NMW 25452.1). It has higher frontal length, loreal height, and loreal width than all the snakes in the western sample, despite not being the longest overall. It is only second to a *P. r. rhodorachis* specimen from Iraq (CAS 157119) in regard to rostral height and width. Apart from these somewhat exceptional measurements, it is not distinguishable from the rest of the western sample other than by color pattern. The *P. r. ladacensis* specimen has wide dorsal collars with very large gaps between them, unlike the more densely dotted patterned morph of *P. r. rhodorachis*. The question of whether *ladacensis* should be raised to a specific status or not is beyond the scope of our study. The geographic gap between the western sample and the distribution range of *P. r. ladacensis* (sensu Schätti *et al*., 2014), and the molecular segregation between the eastern sample and *P. rhodorachis*, suggest that assigning the western sample to *P. r. ladacensis* is highly unlikely.

Seven non-banded specimens we examined are paratypes of *P. saharicus*, which was described from Saint Catherine's Monastery in Sinai, Egypt. The paratypes concur with the latitudinal clinal pattern of the ventral and subcaudal counts (Figs 5a & 5b). We had no tissue samples from topotypes, but two of the samples we used are from an adjacent area (Fig. 6). These two specimens (numbers 35 and 36 in Fig. 6) do not form a distinct clade and are genetically very close to all other members of the western sample. We therefore conclude that both color morphs of the western sample belong to *Platyceps saharicus* Schätti & McCarthy 2004.

Considerations and future research

The fact that most of the specimens examined in this study were preserved prevented the documentation of some color features. The bright yellow color found in the temporal area of non-banded specimens quickly disappears in preservatives, so that museum specimens of both morphs appear pale-grayish.

Our study focused on Israel and its vicinity, including Egypt, but it included only three specimens from Jordan, and only one of those was part of the morphological and molecular analyses, while the other two were only examined from photos. We have no knowledge about the existence (or lack) of populations of *P. saharicus* in Lebanon and Syria. The Jordanian specimen (HUJ 21937) is genetically similar to specimens from Israel. It belongs to the banded morph, while two other Jordanian specimens for which we had only photographs are non-banded. One of those specimens was from Petra (Disi *et al*., 2001, Amr & Disi, 2011) and the other from Wadi Ghuweir (observation from a Facebook group dedicated to trekking in Jordan), both in south-western Jordan. We assume, also following Geniez (2015), that the Jordanian snakes currently assigned to *P. rhodorachis* (Amr & Disi, 2011) actually belong to *P. saharicus*, as there is a wide geographic gap between Jordan and the geographic range of the eastern sample (Schätti *et al*., 2014), and because our genetic results reveal that the Jordanian specimen is indistinguishable from the Israeli ones, while displaying ~10% sequence divergence from eastern snakes of the complex.

The banded morph is probably found on both dark and light soils, but the non-banded, yellowish morph is found almost exclusively on light ones. We tested for an association between the morphs and several environmental variables (mean annual temperature, March-October temperatures, annual precipitation, Net primary productivity, and a dichotomous soil darkness (light or dark) classification (results not shown). Net primary productivity was the only significant predictor of color morph. The distribution of both morphs overlaps the two biomes typical in the region: the banded morph is found mainly in the Mediterranean biome of Israel and Jordan while the non-banded morph is found mainly in the desert biome of Israel, Jordan, and Egypt (Fig. 3). The contact zone of the two morphs occurs around the boundary between the Mediterranean and desert biomes. The banded Jordanian specimen, HUJ21937, has 238 ventrals, more than any other banded snake in our sample, but well within the range of non-banded specimens (Fig. 5A). The number of ventrals fits the latitudinal cline, but the specimen is by far the southern-most banded snake in our sample, with a considerable gap between it and the next banded snakes (Fig. 3). We hypothesize that the presence of a banded specimen in that southern latitude is due to the Mediterranean biome in Jordan continuing further south than it does in Israel. Therefore this specimen has the ventral counts typical of its latitude, but the dorsal color pattern typical of the Mediterranean biome. The existence of color polymorphism alongside the lack of change in meristic characters may indicate a phenotypic response to environmental selection, such as thermoregulation and the need for camouflage (Henderson, 1997).

If our interpretation is correct, then it may indicate that color is adaptive, as the banded morph is darker and may provide better camouflage in the vegetation-rich environment of the Mediterranean biome. Having a darker dorsal tone with a pattern in the Mediterranean biome versus a lighter dorsal tone with the lack of a pattern in the desert is an adaptation shared by other reptilian species in Israel [e.g., *Chalcides ocellatus* (Forskål, 1775)*, Eryx jaculus* (Linnaeus, 1758), and *Psammophis schokari* (Forskal, 1775); see Bar & Haimovitch, 2013].

The Jordanian specimen, HUJ 21937 (with many ventrals and a dark, banded pattern), suggests that there is no pleiotropic effect between the ventral count and the dorsal color pattern. This conclusion is further supported by the clinal pattern demonstrated by the ventral count versus the dichotomous nature of the dorsal coloration.

We did not find any melanistic specimens among the western sample. Two specimens in the Steinhardt Museum (SNHM 13753 and SNHM 13833) both from Tiran Island, Sinai, have very dark dorsum and melanin concentrations on the ventrals and the subcaudals. They have fewer ventrals (209 and 215 respectively) than any specimen of the western sample (minimum 217), and are in disagreement with the clinal increase in ventral counts towards lower latitudes. Those melanistic specimens resemble the gray color morph of *P. rhodorachis* that is found in the eastern Arabian Peninsula, and *P. r. subniger* that is found in the horn of Africa (Perry 2012; Schätti *et al*., 2014). A gray *P. rhodorachis*, CAS 251164 (from Ad Dakhiliyah Governorate, Oman), was included in our molecular analysis (Fig. 6) and emerged as the sister group of a clade containing both the western sample (*P. saharicus*) and *P. rogersi*. We think the specimens from Tiran Island may belong to this gray color morph of *P. rhodorachis*. Whether or not this gray color morph (CAS 251164) is indeed *P. rhodorachis* or belongs to a distinct species requires further investigation. Other specimens of *P. rhodorachis,* from Iran and Turkmenistan, do not cluster with this specimen (Fig. 6).

Schätti *et al*. (2012) downgraded *Platyceps rogersi* to a subspecific rank, *P. karelini rogersi*. Our tree topology (Fig. 6) places *P. saharicus* as the sister group of *P. rogersi*, while *P. rhodorachis* (CAS 251164) is the sister taxon of both *P. saharicus* and *P. rogersi*. *Platyceps karelini* is placed as a sister group to a clade containing all these three taxa (*rhodorachis, saharicus*, and *rogersi*). The *12S* sequence divergence analysis (Appendix 7) suggests that the closest species to *P. rogersi* is *P. saharicus*. In the *cytb* gene fragment, *P. saharicus* is also closer to *p. rogersi than is P. karelini*. Therefore, we suggest that further research is needed regarding the taxonomic rank of *P. rogersi*, as its current subspecific rank under *P. karelini* is not supported. This taxonomy was also adopted by Geniez (2015) on the basis of the constant differences found between the coloration patterns of these two taxa.

Our findings suggest that the banded and the non-banded color morphs found in Israel and its vicinity belong to a single member of the *P. rhodorachis* complex - in this case *P. saharicus*. This species is morphologically dimorphic, with two color patterns, which may be adaptations to the environmental attributes of their habitats and biomes: a yellowish morph in the southern desert areas and a grayish one in the more mesic, Mediterranean regions. We suspect that this may play a role in camouflage. The ventral and subcaudal counts do not enable classification of the morphs into two species. Rather, they are best explained as a clinal latitudinal pattern. The two color morphs form a monophyletic clade, as far as can be deduced from *COI*, *cytb*, and the *12S* gene fragments (Fig. 6). This clade forms a sister group to *P. rogersi*, despite its morphological similarities to *P. rhodorachis* (Fig. 6). The three *P. rhodorachis* molecular samples included in this study do not form a monophyletic clade (Fig. 6). Future research is needed regarding the taxonomic status of the *P. rhodorachis* population from Arabia and the Horn of Africa, as they may belong to a different species than those in Iraq and eastwards (Fig. 1).

Acknowledgements

We would like to thank Erez Maza (SMNH) for his help in the fieldwork and for allowing us access to specimens under his care. We thank Boaz Shacham (HUJ) for allowing us access to specimens under his care, Patrick Campbell (BMNH), Jens Vindum (CAS), Alan Resetar (FMNH), Patrick Semal (IRSNB), Sébastien Bruaux (IRSNB), Tom Geerinckx (IRSNB), Nicolas Vidal (MNHN), Carol Spencer (MVZ), Georg Gassner (NMW) and Ursula Bott (ZFMK) for sending us photographs and specimens under their care. We thank Karin Tamar for her help regarding molecular analyses and in the fieldwork. We are grateful to Aviad Bar for valuable discussion and help in fieldwork. We thank Alex Slavenko, Anat Feldman, David David, Enav Vidan, Gavin Stark, Guy Sion, Hamutal Friedman, Lior Davis, Maria Novosolov, Michaela Kolker, Oliver Tallowin, Rachel Schwartz, Simon Jamison, and Yuval Itescu for valuable discussions and help in the field. We thank Philippe Geniez and two anonymous reviewers for their helpful remarks. Naomi Paz kindly edited the English. Guy Sinaiko was supported by an MSc. scholarship from the School of Zoology, Tel-Aviv University.

References

Amr, Z.S. & Disi, A.M. (2011) Systematics, distribution and ecology of the snakes of Jordan. *Vertebrate Zoology*, 61 (2), 179–266.

Anderson, J. (1871) A list of the reptilian accession to the Indian Museum, Calcutta, from 1865 to 1870, with a description of some new species. *Journal of the Asiatic Society of Bengal*, 40 (2), 12–39.

Anderson, J. (1895) On a collection of reptiles and batrachians made by Colonel Yerbury at Aden and its neighbourhood. *Proceedings of the Zoological Society of London*, 1895 (3), 635–663.

Arnold, T.W. (2010) Uninformative parameters and model selection using Akaike's Information Criterion. *Journal of Wildlife Management*, 74 (6), 1175–1178.
https://doi.org/10.1111/j.1937-2817.2010.tb01236.x

Arbel, A. (Ed.) (1984) *Plants & animals of the land of Israel, An Illustrated Encyclopedia*. Volume 5. Reptiles & amphibians. Society for the Protection of Nature & Ministry of Defence Publishing House, Jerusalem, 244 pp. [in Hebrew]

Bar, A. & Haimovitch, G. (2013) *A field guide to reptiles and amphibians of Israel*. Pazbar Publishing house, 249 pp. [in Hebrew]

Barash, A. & Hoofien, J.H. (1961) *Reptiles of Israel*. Hakibbutz Hameuchad Publishing House, Tel Aviv, 179 pp. [in Hebrew]

Bodenheimer, F.S. (1935) *Animal life in Palestine*. L. Mayer, Jerusalem, 506 pp.

Bodenheimer, F.S. (1953) *Animal Life in the Land of Israel*. Dvir Publishing House, Or Yehuda, 436 pp. [in Hebrew]

Boulenger, G.A. (1893) *Catalogue of the Snakes in the British Museum*. Volume I. Trustees of The British Museum (Natural

History), London, xiii + 448 pp.
Bouskila, A. & Amitai, P. (2001) *A Handbook of the Reptiles and Amphibians of Israel*. Keter Publishing House Limited, Jerusalem, 345 pp. [in Hebrew]
Bryson, R.W., Murphy, R.W., Lathrop, A. & Lazcano?Villareal, D. (2011) Evolutionary drivers of phylogeographical diversity in the highlands of Mexico: a case study of the *Crotalus triseriatus* species group of montane rattlesnakes. *Journal of Biogeography*, 38 (4), 697–710.
https://doi.org/10.1111/j.1365-2699.2010.02431.x
Burbrink, F.T., Lawson, R. & Slowinski, J.B. (2000) Mitochondrial DNA phylogeography of the polytypic North American rat snake (*Elaphe obsoleta*): a critique of the subspecies concept. *Evolution*, 54 (6), 2107–2118.
https://doi.org/10.1111/j.0014-3820.2000.tb01253.x
Calder, W.A. (1984) *Size, function and life history*. Harvard University Press, Cambridge, 448 pp.
Cox, N., Chanson, J. & Stuart, S. (Compilers) (2006) *The status and distribution of reptiles and amphibians of the Mediterranean Basin*. IUCN, Gland & Cambridge, v + 42 pp.
Darriba, D., Taboada, G.L., Doallo, R. & Posada, D. (2012) jModelTest 2: more models, new heuristics and parallel computing. *Nature methods*, 9 (8), 772–772.
https://doi.org/10.1038/nmeth.2109
Disi, A., Modry, D., Necas, P. & Rifai L. (2001) *Amphibians and reptiles of the Hashemite Kingdom of Jordan: an atlas and field guide. Vol. 9*. Chimaira, Frankfurt, 408 pp.
Dowling, H.G. (1950) Studies of the black swamp snake, *Seminatrix pygaea* (Cope) with description of two new subspecies. *Miscellaneous Publications from the Museum of Zoology University of Michigan*, 76, 1–38.
Dowling, H.G. (1951) A proposed standard system of counting ventrals in snakes. *British Journal of Herpetology*, 1, 97–99.
Drummond, A.J. & Rambaut, A. (2007) BEAST: Bayesian evolutionary analysis by sampling trees. *BMC evolutionary biology*, 7 (1), 214.
https://doi.org/10.1186/1471-2148-7-214
Edwards, S., Vanhooydonck, B., Herrel, A., Measey, G.J. & Tolley, K.A. (2012) Convergent evolution associated with habitat decouples phenotype from phylogeny in a clade of lizards. *PloS ONE*, 7 (12), e51636.
https://doi.org/10.1371/journal.pone.0051636
Ewert, M.A. (1985) *Biology of the Reptilia. Vol. 14. Development A*. John Wiley & Sons, New York, xii + 763 pp.
Feldman, A. & Meiri, S. (2013) Length–mass allometry in snakes. *Biological Journal of the Linnean Society*, 108 (1), 161–172.
https://doi.org/10.1111/j.1095-8312.2012.02001.x
Felsenstein, J. (1985) Confidence limits on phylogenies: an approach using the bootstrap. *Evolution*, 39 (4), 783–791.
https://doi.org/10.1111/j.1558-5646.1985.tb00420.x
Geniez, P. & Gauthier, Y. (2008) On the distribution of *Platyceps saharicus* (Reptilia: Colubridae) in the Sahara. *Salamandra*, 44 (4), 179–180.
Geniez, P. (2015) *Serpents d'Europe, d'Afrique du Nord et du Moyen-Orient*. Delachaux et Niestlé, Lausanne, 380 pp.
Goujon, M., McWilliam, H., Li, W., Valentin, F., Squizzato, S., Paern, J. & Lopez, R. (2010) A new bioinformatics analysis tools framework at EMBL–EBI. *Nucleic acids research*, 38, W695–W699.
https://doi.org/10.1093/nar/gkq313
Guindon, S. & Gascuel, O. (2003) A simple, fast, and accurate algorithm to estimate large phylogenies by maximum likelihood. *Systematic biology*, 52 (5), 696–704.
https://doi.org/10.1080/10635150390235520
Günther, A. (1865) Report on a collection of reptiles and fishes from Palestine. *Proceedings of the Zoological Society of London*, 1864, 488–493.
Günther, A. (1878) Specimens of reptiles presented by Captain Burton to the British Museum. *In*: Burton, R. (Ed.), *The Gold Mines of Midian and the ruined Midianite cities*. C. Kegan Paul & Co., London, xvi + 395 pp.
Harris, D.J. (2002) Reassessment of comparative genetic distance in reptiles from the mitochondrial cytochrome b gene. *Herpetological Journal*, 12 (2), 85–87.
Helbig, A.J., Knox, A.G., Parkin, D.T., Sangster, G. & Collinson, M. (2002) Guidelines for assigning species rank. *Ibis*, 144 (3), 518–525.
https://doi.org/10.1046/j.1474-919X.2002.00091.x
Henderson, R.W. (1997) A taxonomic review of the *Corallus hortulanus* complex of Neotropical tree boas. *Caribbean Journal of Science*, 33, 198–221.
Huelsenbeck, J.P. & Rannala, B. (2004) Frequentist properties of Bayesian posterior probabilities of phylogenetic trees under simple and complex substitution models. *Systematic biology*, 53 (6), 904–913.
https://doi.org/10.1080/10635150490522629
Huelsenbeck, J.P. & Ronquist, F. (2001) MRBAYES: Bayesian inference of phylogenetic trees. *Bioinformatics*, 17 (8), 754–755.
https://doi.org/10.1093/bioinformatics/17.8.754
Inger, R.F. & Clark, P.J. (1943) Partition of the genus *Coluber*. *Copeia*, 1943 (3), 141–145.
https://doi.org/10.2307/1438603
Kelly, C.M., Barker, N.P., Villet, M.H., Broadley, D.G. & Branch, W.R. (2008) The snake family Psammophiidae (Reptilia:

Serpentes): phylogenetics and species delimitation in the African sand snakes (*Psammophis Boie*, 1825) and allied genera. *Molecular Phylogenetics and Evolution*, 47 (3), 1045–1060.
https://doi.org/10.1016/j.ympev.2008.03.025

Kramer, E. & Schnurrenberger, H. (1963) Systematik, Verbreitung und Ökologie der Libyschen Schlangen. *Revue Suisse de Zoologie*, 70 (3), 453–568.
https://doi.org/10.5962/bhl.part.75250

Laszlo, J. (1975) Probing as a practical method of sex recognition in snakes. *International Zoo Yearbook*, 15 (1), 178–179.
https://doi.org/10.1111/j.1748-1090.1975.tb01393.x

Lindell, L.E., Forsman, A. & Merilä, J. (1993) Variation in number of ventral scales in snakes: effects on body size, growth rate and survival in the adder, *Vipera berus*. *Journal of Zoology*, 230 (1), 101–115.
https://doi.org/10.1111/j.1469-7998.1993.tb02675.x

Mallet, J. (1995) A species definition for the modern synthesis. *Trends in Ecology & Evolution*, 10 (7), 294–299.
https://doi.org/10.1016/0169-5347(95)90031-4

Manier, M.K. (2004) Geographic variation in the long?nosed snake, *Rhinocheilus lecontei* (Colubridae): beyond the subspecies debate. *Biological Journal of the Linnean Society*, 83 (1), 65–85.
https://doi.org/10.1111/j.1095-8312.2004.00373.x

Mayr, E. (1942) *Systematics and the origin of species from the viewpoint of a zoologist*. Columbia University Press, New York, xiv + 334 pp.

McDiarmid, R.W., Foster, M.S., Guyer, C., Gibbons, J.W. & Chernoff, N. (2012) *Reptile biodiversity: standard methods for inventory and monitoring*. University of California Press, Berkeley, xii + 424 pp.

Mendelson III, J.R., Barclay, M.V., Geiser, M. & Streicher, J.W. (2016) The taxonomic status of *Bufo intermedius* Günther, 1858: forensic entomology confirms what was long suspected from morphology. *Copeia*, 104 (3), 697–701.
https://doi.org/10.1643/CH-16-422

Nagy, Z.T., Lawson, R., Joger, U. & Wink, M. (2004) Molecular systematics of racers, whipsnakes and relatives (Reptilia: Colubridae) using mitochondrial and nuclear markers. *Journal of Zoological Systematics and Evolutionary Research*, 42 (3), 223–233.
https://doi.org/10.1111/j.1439-0469.2004.00249.x

Nylander, J.A., Wilgenbusch, J.C., Warren, D.L. & Swofford, D.L. (2007) AWTY (are we there yet?): a system for graphical exploration of MCMC convergence in Bayesian phylogenetics. *Bioinformatics*, 24 (4), 581–583.
https://doi.org/10.1093/bioinformatics/btm388

Olden, J.D., Lawler, J.J. & Poff, N.L. (2008) Machine learning methods without tears: a primer for ecologists. *The Quarterly review of biology*, 83 (2), 171–193.
https://doi.org/10.1086/587826

Olson, D.M., Dinerstein, E., Wikramanayake, E.D., Burgess, N.D., Powell, G.V., Underwood, E.C., D'amico, J.A., Itoua, I., Strand, H.E., Morrison, J.C. & Loucks, C.J. (2001) Terrestrial Ecoregions of the World: A New Map of Life on Earth: A new global map of terrestrial ecoregions provides an innovative tool for conserving biodiversity. *BioScience*, 51 (11), 933–938.
https://doi.org/10.1641/0006-3568(2001)051[0933:TEOTWA]2.0.CO;2

Osgood, D.W. (1978) Effects of temperature on the development of meristic characters in *Natrix fasciata*. *Copeia*, 1978, 33–47.
https://doi.org/10.2307/1443819

Perry, G. (2012) On the Appropriate Names for Snakes Usually Identified as *Coluber rhodorachis* (Jan, 1865) or Why Ecologists Should Approach the Forest of Taxonomy with Great Care. *IRCF Reptiles & Amphibians*, 19 (20), 90–100.

Peters, H.R. (1983) The ecological implications of body size. Cambridge University Press, New York, 329 pp.
https://doi.org/10.1017/CBO9780511608551

Pincheira-Donoso, D. & Meiri, S. (2013) An intercontinental analysis of climate-driven body size clines in reptiles: no support for patterns, no signals of processes. *Evolutionary Biology*, 40, 562–578.
https://doi.org/10.1007/s11692-013-9232-9

Pyron, R.A., Burbrink, F.T. & Wiens, J.J. (2013) A phylogeny and revised classification of Squamata, including 4161 species of lizards and snakes. *BMC Evolutionary Biology*, 13 (1), 93.
https://doi.org/10.1186/1471-2148-13-93

R Core Team (2016) R: A language and environment for statistical computing. R Foundation for Statistical Computing, Vienna. Available from: https://www.r-project.org/ (accessed 10 January 2018)

Razzetti, E., Faiman, R. & Werner, Y.L. (2007) Directional asymmetry and correlation of tail injury with left-side dominance occur in Serpentes (Sauropsida). *Zoomorphology*, 126 (1), 31–43.
https://doi.org/10.1007/s00435-007-0028-2

Ronquist, F. & Huelsenbeck, J.P. (2003) MrBayes 3: Bayesian phylogenetic inference under mixed models. *Bioinformatics*, 19 (12), 1572–1574.
https://doi.org/10.1093/bioinformatics/btg180

Sanders, K.L. Rasmussen, A.R., Elmberg, J., Silva, A., Guinea, M.L. & Lee, M.S. (2013) Recent rapid speciation and ecomorph divergence in Indo?Australian sea snakes. *Molecular ecology*, 22 (10), 2742–2759.
https://doi.org/10.1111/mec.12291

Schätti, B. & McCarthy, C. (2004) Saharo-Arabian racers of the *Platyceps rhodorachis* complex: description of a new species (Reptilia: Squamata: Colubrinae). *Revue suisse de Zoologie*, 111 (4), 691–705.
https://doi.org/10.5962/bhl.part.80263

Schätti, B., Tillack, F. & Kucharzewski, C. (2014) *Platyceps rhodorachis* (Jan, 1863)–a study of the racer genus *Platyceps* BLYTH, 1860 east of the Tigris (Reptilia: Squamata: Colubridae). *Vertebrate Zoology*, 64, 297–405.

Schätti, B. & Utiger, U. (2001) Hemerophis, a new genus for *Zamenis socotrae* Günther, and a contribution to the phylogeny of Old World racers, whip snakes, and related genera (Reptilia: Squamata: Colubrinae). *Revue suisse de Zoologie*, 108 (4), 919–948.
https://doi.org/10.5962/bhl.part.80170

Sievers, F., Wilm, A., Dineen, D., Gibson, T.J., Karplus, K., Li, W., Lopez, R., McWilliam, H., Remmert, M., Söding, J. & Thompson, J.D. (2011) Fast, scalable generation of high?quality protein multiple sequence alignments using Clustal Omega. *Molecular systems biology*, 7 (1), 539.
https://doi.org/10.1038/msb.2011.75

Silvestro, D. & Michalak, I. (2012) raxmlGUI: a graphical front-end for RAxML. *Organisms Diversity & Evolution*, 12 (4), 335–337.
https://doi.org/10.1007/s13127-011-0056-0

Sindaco, R., Venchi, A. & Grieco, C. (2013) *The Reptiles of the western Palearctic. 2. Annotated checklist and distributional atlas of the snakes of Europe, North Africa. Middle East and Central Asia*. Edizioni Belvedere, Latina, 543 pp.

The reptiles of the Western Palearctic, vol. 2. Annotated checklist and distributional atlas of the snakes of Europe, North Africa, Middle East and Central Asia. Belvedere, Latina, Italy.

Stamatakis, A. (2014) RAxML version 8: a tool for phylogenetic analysis and post-analysis of large phylogenies. *Bioinformatics*, 30 (9), 1312–1313.
https://doi.org/10.1093/bioinformatics/btu033

Tamura, K., Peterson, D., Peterson, N., Stecher, G., Nei, M. & Kumar, S. (2011) MEGA5: molecular evolutionary genetics analysis using maximum likelihood, evolutionary distance, and maximum parsimony methods. *Molecular biology and evolution*, 28 (10), 2731–2739.
https://doi.org/10.1093/molbev/msr121

Tristram, H.B. (1884) *The survey of Western Palestine: the fauna and flora of Palestine*. Committee of the Palestine Exploration Fund, London, xxii + 455 pp.
https://doi.org/10.5962/bhl.title.7594

Uetz, P. (2018) The Reptile Database. Available from: http://www.reptile-database.org/ (accessed 10 January 2018)

Werner, F. (1910) Neue oder seltenere Reptilien des Musée Royal d'Histoire Naturelle de Belgique in Brüssel. *Zoologische Jahrbuecher Abteilung fuer Systematik Oekologie und Geographie der Tiere*, 28, 263–288.
https://doi.org/10.5962/bhl.part.17594

Werner, Y.L. (1988) Herpetofaunal survey of Israel (1950-85), with comments on Sinai and Jordan and on zoogeographical heterogeneity. *Monographiae biologicae*, 62, 355–388.

Werner, Y.L. (1995) *A guide to the reptiles and amphibians of Israel*. Nature Reserves Authority—Yefe-Nof Library, Jerusalem, 86 pp.

Werner, Y.L. (1998) The desert herpetofauna in and near Israel: a personal review of advances (1986–1997), with new data (Amphibia; Reptilia). *Faunistische Abhandlungen Staatliches Museum für Tierkunde Dresden*, 21, 149–161.

Werner, Y.L. (2016) *Reptile life in the land of Israel, with comments on adjacent regions*. Chimaira, Frankfurt, 494 pp.

Wheeler, B. & Torchiano, M. (2016) lmPerm: Permutation Tests for Linear Models, R package version 2.1.0. Available from: https://CRAN.R-project.org/package=lmPerm (accessed 10 January 2018)

Wiens, J.J. & Servedio, M.R. (2000) Species delimitation in systematics: inferring diagnostic differences between species. *Proceedings of the Royal Society of London B: Biological Sciences*, 267 (1444), 631–636.
https://doi.org/10.1098/rspb.2000.1049

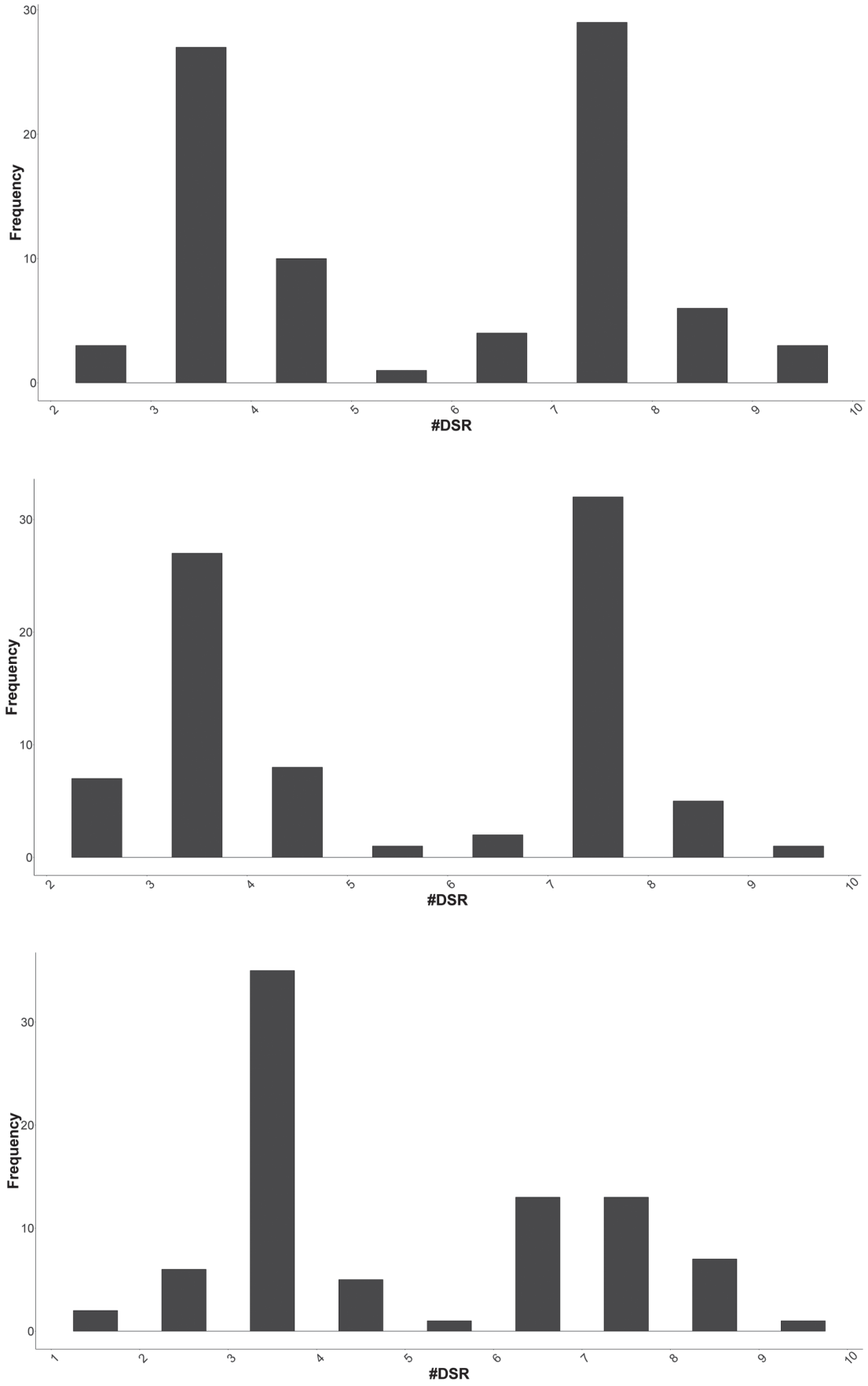

FIGURE S1. Bimodal histograms of characters in the western sample. A) Dorsal location of dorsal scale rows reduction from 19 to 18 rows. BM13 DSRDL 19-18 B) Dorsal location of dorsal scale rows reduction from 18 to 17 rows C) Dorsal location of dorsal scale rows reduction from 16 to 15 rows.

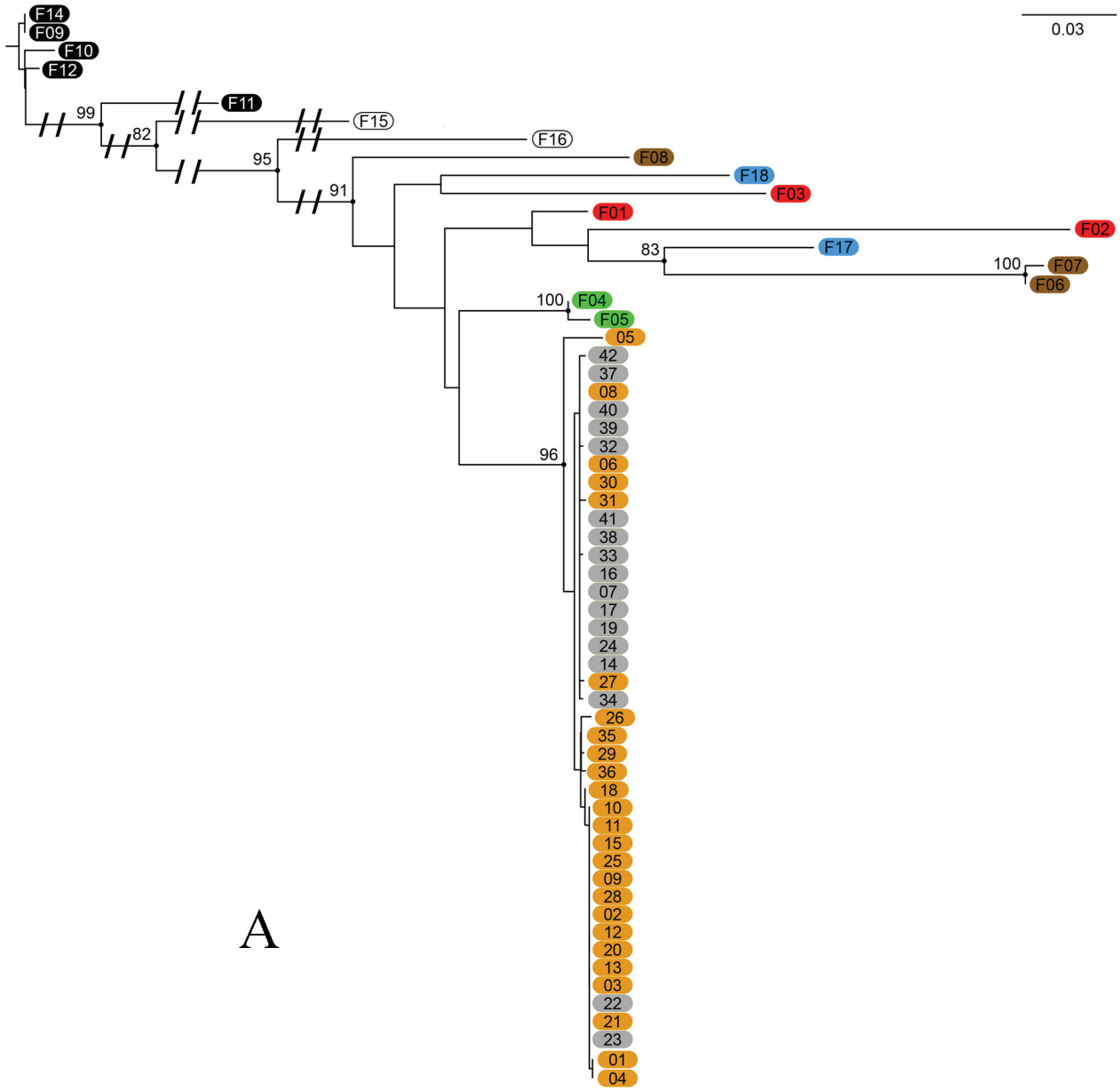

FIGURE S2. A) Consensus tree based on concatenated *cytb* and *12S* gene fragments. Support values are bootstrap values of a maximum likelihood analysis. Values lower than 80 are not shown. B) Consensus tree based on *cytb* gene fragment. Support values are posterior probabilities of a Bayesian inference analysis. Values lower than 0.9 are not shown. C) Consensus tree based on *cytb* gene fragment. Support values are bootstrap values of a maximum likelihood analysis. Values lower than 80 are not shown. D) Consensus tree based on *12S* gene fragment. Support values are posterior probabilities of a Bayesian inference analysis. Values lower than 0.9 are not shown. E) Consensus tree based on *12S* gene fragment. Support values are bootstrap values of a maximum likelihood analysis. Values lower than 80 are not shown. Branches which are not shown to full length are indicated by / /. Gray: banded morph (western sample). Yellow: non-banded morph (western sample). Red: *P. rhodorachis* (eastern sample). Green: *P. rogersi*. Blue: *P. karelini*. Brown: *P. collaris*. White: *Hemorrhois nummifer*. Black: *Spalerosophis diadema*.

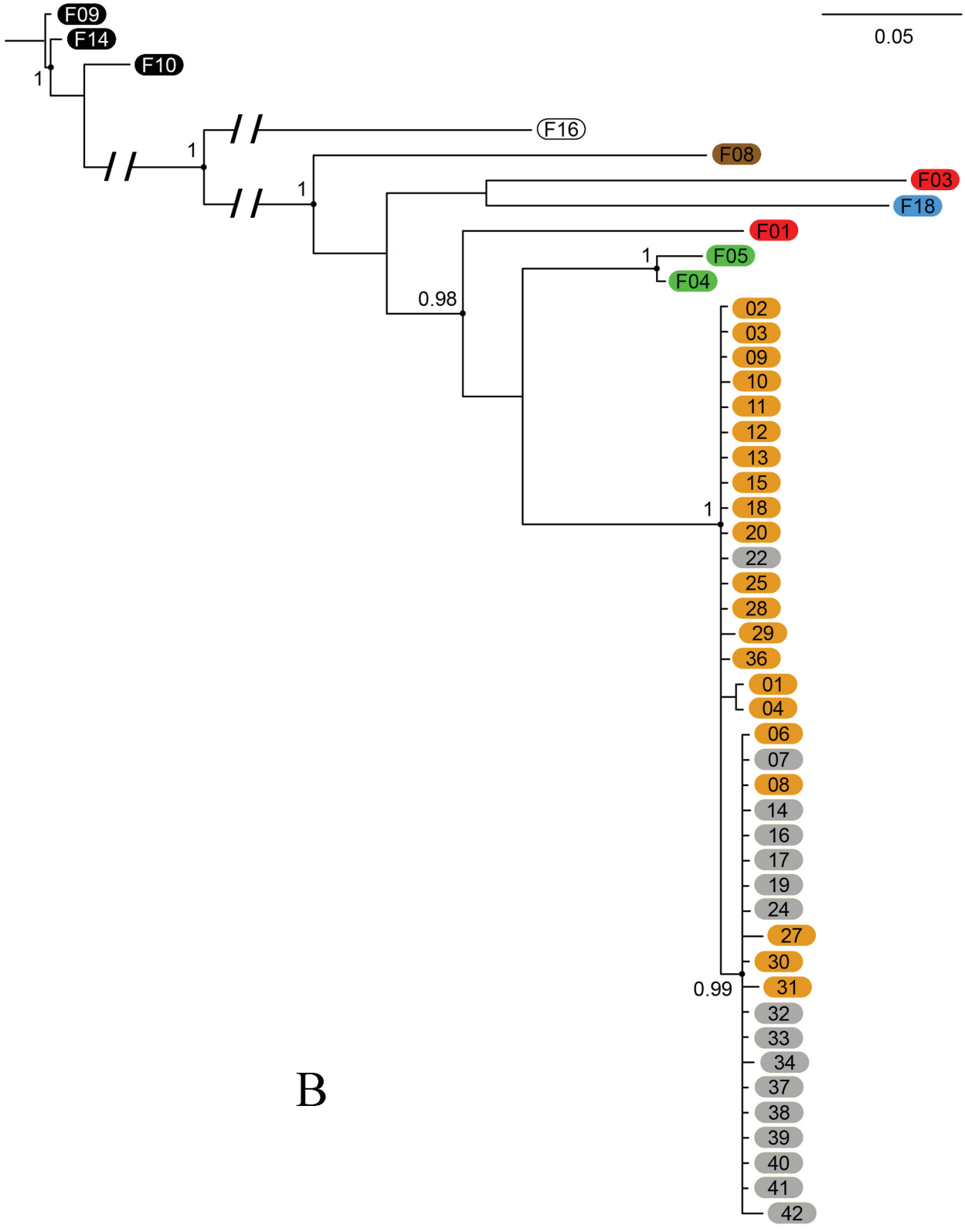
0.05
F09
F14
F10
F16
F08
F03
F18
F01
F05
F04
02
03
09
10
11
12
13
15
18
20
22
25
28
29
36
01
04
06
07
08
14
16
17
19
24
27
30
31
32
33
34
37
38
39
40
41
42
1
1
1
1
0.98
0.99
B

FIGURE S2B.

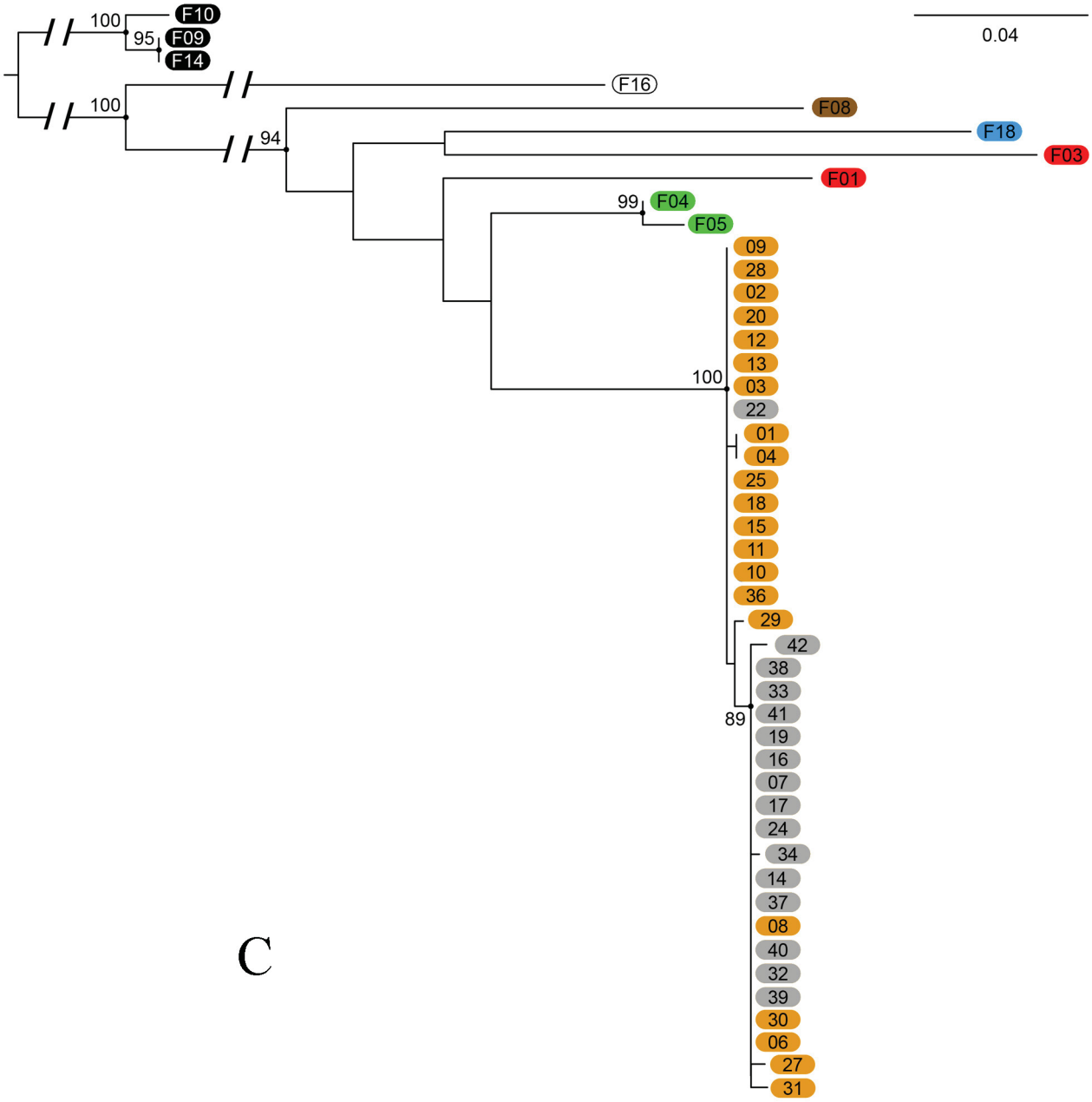
0.04
100
95
F10
F09
F14
100
F16
94
F08
F18
F03
F01
99
F04
F05
09
28
02
20
12
13
100
03
22
01
04
25
18
15
11
10
36
29
42
38
33
89
41
19
16
07
17
24
34
14
37
08
40
32
39
30
06
27
31
C

FIGURE S2C.

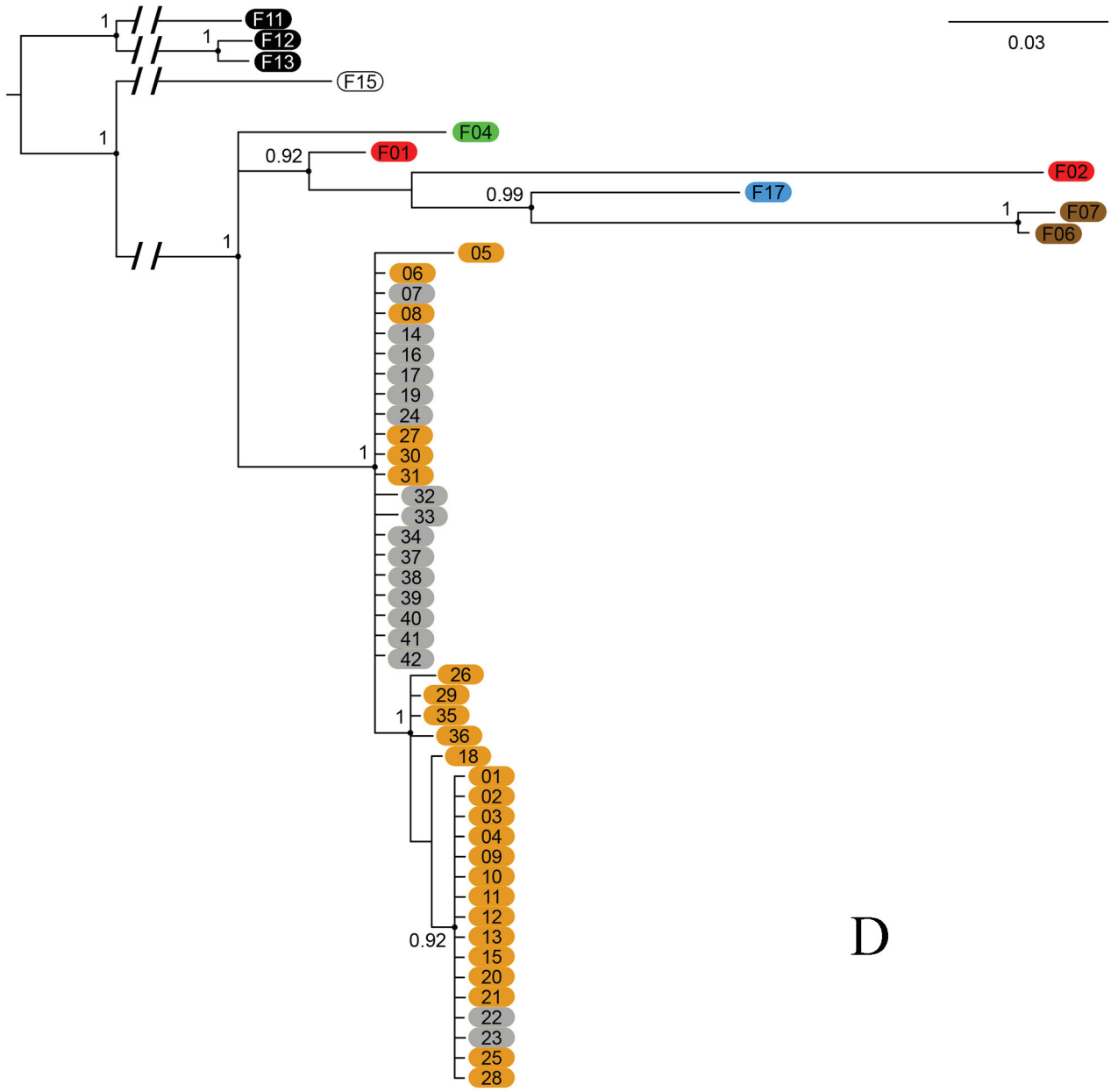
0.03
F11
F12
F13
F15
F04
F01
F02
F17
F07
F06
05
06
07
08
14
16
17
19
24
27
30
31
32
33
34
37
38
39
40
41
42
26
29
35
36
18
01
02
03
04
09
10
11
12
13
15
20
21
22
23
25
28
1
0.92
0.99
D

FIGURE S2D.

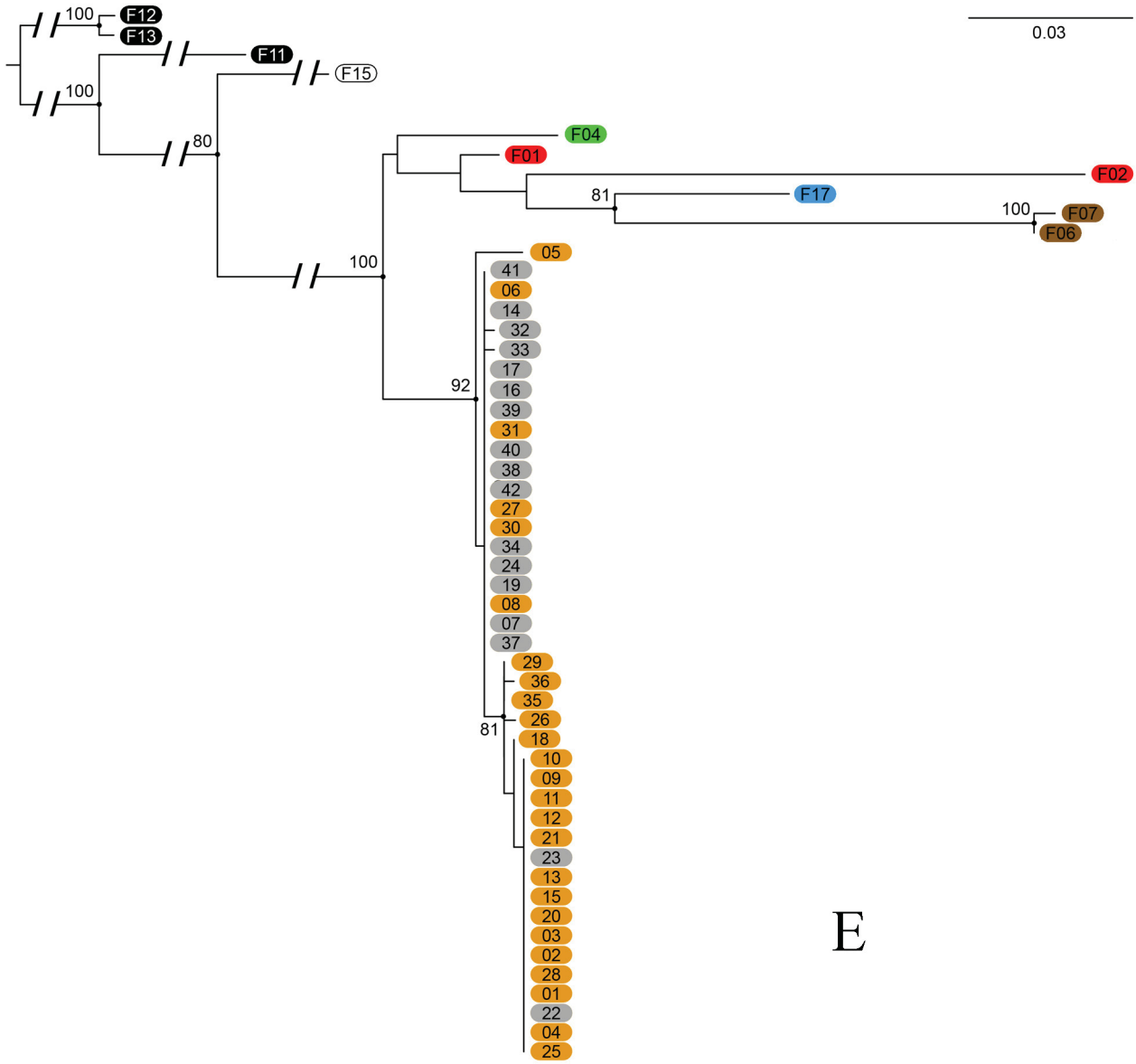
0.03
100
F12
F13
F11
F15
100
80
F04
F01
F02
81
F17
100
F07
F06
100
05
41
06
14
32
33
17
92
16
39
31
40
38
42
27
30
34
24
19
08
07
37
29
36
35
81
26
18
10
09
11
12
21
23
13
15
20
03
02
28
01
22
04
25
E

FIGURE S2E.

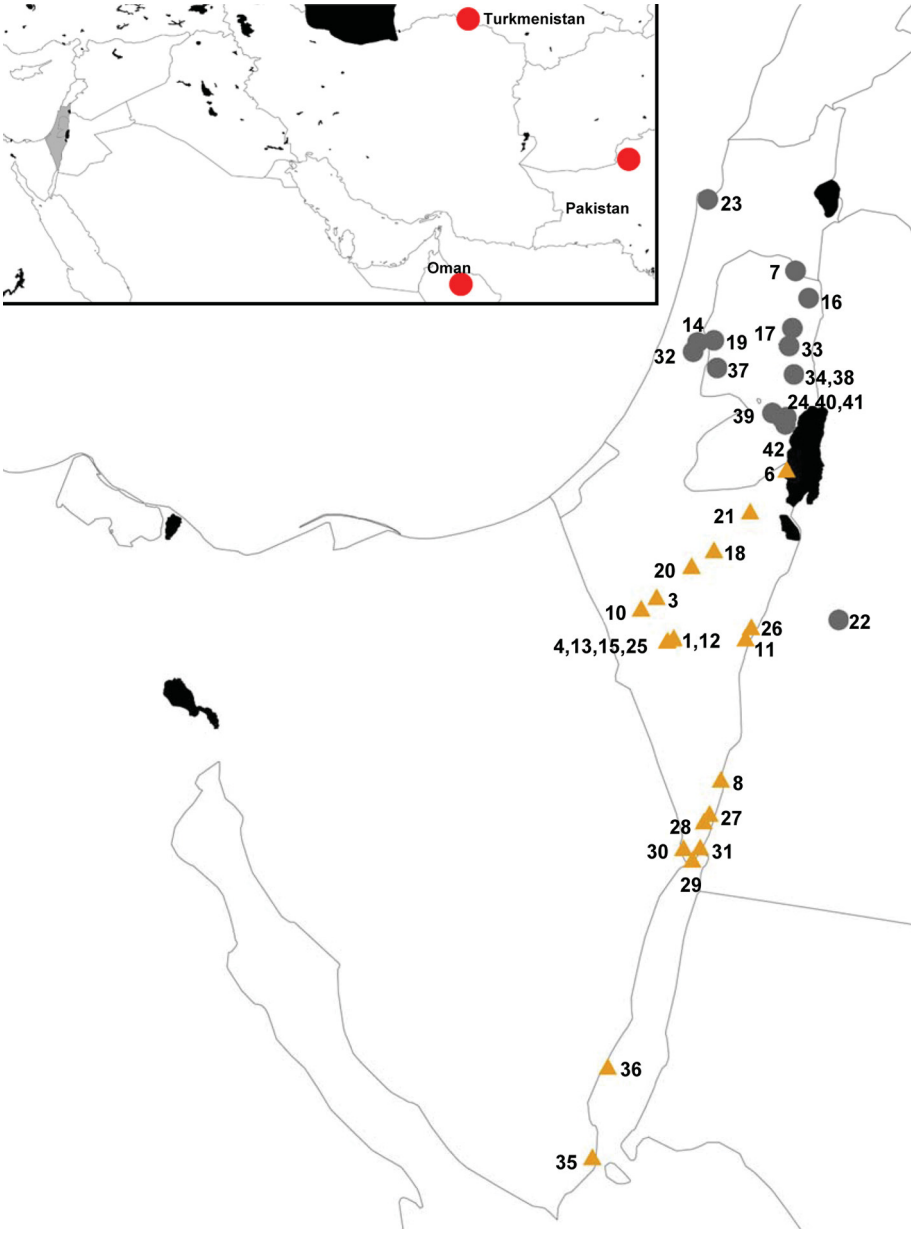

FIGURE S3. A map of all western and eastern specimens examined for molecular analysis in this study. Specimen numbering is in accordance with the list in Appendix1.

APPENDIX 1. Material examined. Geographic coordinates are expressed in decimal degrees as "latitude, longitude" (e.g. 31.46, 35.38 mean 31.46° N, 35.38° W); * indicates whether a specimen was examined for morphology and whether *COI*, *12S* and *cytb* gene fragments were amplified. All FMNH specimens were examined only by photographs. Institute acronyms used: The Steinhardt Museum of Natural History (SNHM), Tel Aviv, Israel; The Hebrew University of Jerusalem (HUJ), Jerusalem, Israel; BMNH, Natural History Museum, London, U.K.; CAS, California Academy of Sciences, San Francisco, California, U.S.A.; FMNH, Field Museum of Natural History, Chicago, Illinois, U.S.A.; HLMD, Hessischen Landesmuseum Darmstadt, Darmstadt, Germany; IRSNB, Institut Royal des Sciences Naturelles de Belgique, Brussels, Belgium; MHNG, Muséum d'histoire naturelle, Genève, Switzerland; MNHN, Muséum National d'Histoire naturelle, Paris, France; MVZ, Museum of Vertebrate Zoology, University of California at Berkeley, California, U.S.A.; NMW, Naturhistorisches Museum, Wien, Austria; ROM, Royal Ontario Museum, Department of Natural History, Toronto, Ontario, Canada; SH, Tissue collection of Notker Helfenberger; ZFMK, Zoologisches Forschungsmuseum Alexander König, Bonn, Germany; ZISP, Zoological Institute, Russian Academy of Sciences, St. Petersburg, Russia.
WNB = Western non-banded *Platyceps saharicus.*
WB = Western banded *Platyceps saharicus*.

Species / Morph	Voucher	Genbank accession	Morphology	Genetic sample #	*COI*	*12S*	*cytb*	Location	Latitude	Longitude
WB	SMNH 15670	MF767363, MF767312, MF767374	*	7	*	*	*	Israel, Merav	32.44	35.44
WB	SMNH 17188	MF767367, MF767319, MF767381	*	14	*	*	*	Israel, Rosh haa'in	32.09	34.95
WB	SMNH 17216	MF767359, MF767321, MF767383	*	16	*	*	*	Israel, Samaria, Maskiyyot, Road no. 578	32.31	35.5
WB	SMNH 17217	MF767361, MF767322, MF767384	---	17	*	*	*	Israel, Samaria, Mekhora, Road no. 578	32.16	35.42
WB	SMNH 17243	MF767360, MF767324, MF767386	*	19	*	*	*	Israel, Elkana	32.1	35.03
WB	HUJ 21937	MF767353, MF767327, MF767388	*	22	*	*	*	Jordan, Jordan: Wadi Gargur, 2km SW of Bussier, N. Edom (200m ASL)	30.71	35.65
WB	HUJ 22046	MF767328	*	23	---	*	---	Israel, Haifa: Ha-Rofe street	32.8	35
WB	SMNH 17354	MF767329, MF767389	*	24	---	*	*	Israel, Bikaat-hurkanya	31.72	35.39
WB	SMNH 17807	MF767338, MF767397	*	32	---	*	*	Israel, Rinatya	32.04	34.93
WB	SMNH 17808	MF767339, MF767398	*	33	---	*	*	Israel, Ma'ale Efrayim	32.07	35.4
WB	SMNH 17813	MF767340, MF767399	*	34	---	*	*	Israel, Ein-qedem farm, Mevo'ot Yericho	31.93	35.43
WB	SMNH 17818	MF767344, MF767401	*	37	---	*	*	Israel, Nili	31.96	35.05
WB	SMNH 17848	MF767345, MF767402	*	38	---	*	*	Israel, Ein-qedem farm, Mevo'ot Yericho	31.93	35.43
WB	SMNH 17850	MF767346, MF767403	*	39	---	*	*	Israel, Kedar	31.74	35.32

……continued on the next page

APPENDIX 1. (Continued)

Species / Morph	Voucher	Genbank accession	Morphology	Genetic sample #	*COI*	*12S*	*cytb*	Location	Latitude	Longitude
WB	SMNH 17851	MF767347, MF767404	*	40	---	*	*	Israel, Hurkania	31.71	35.37
WB	SMNH 17852	MF767348, MF767405	*	41	---	*	*	Israel, Hurkania	31.71	35.37
WB	SMNH 17853	MF767349, MF767406	*	42	---	*	*	Israel, Hurkania	31.68	35.38
WB	HUJ 16412	---	*	---	---	---	---	Israel, Mizpe Shalem	31.56	35.4
WB	HUJ 16424	---	*	---	---	---	---	Israel, Jericho-'Ein Faskha road: N of Qalya	31.76	35.49
WB	HUJ 16425	---	*	---	---	---	---	Israel, Jordan Valley: 5km N of Yericho	31.9	35.46
WB	HUJ 16590	---	*	---	---	---	---	Israel, enait from 'Arqan um Zafa	32.07	35.42
WB	HUJ 16677	---	*	---	---	---	---	Israel, nr. Pazael	32.05	35.42
WB	HUJ 16855	---	*	---	---	---	---	Unknown location	---	---
WB	HUJ 16961	---	*	---	---	---	---	Israel, Ma'ale Adumim ("Stn.1")	31.77	35.3
WB	HUJ 16964	---	*	---	---	---	---	Israel, Nahal Soreq: pine forest near sewage, 1km E jct road & rail	31.93	34.7
WB	HUJ 20863	---	*	---	---	---	---	Israel, 500m S to Ein Fashkha	31.71	35.44
WB	HUJ 20985	---	*	---	---	---	---	Israel, Mt. Gilbo'a: Ma'ale Merav rd.	32.44	35.44
WB	HUJ 21015	---	*	---	---	---	---	Israel, E Mifgash HaBiq'a: Yanshuf Milit. Pos., 500m W Jordan River	32.04	35.51
WB	HUJ 21208	---	*	---	---	---	---	Israel, Ari'el	32.1	35.17
WB	HUJ 21599	---	*	---	---	---	---	Israel, Qeydar settlement, S of Ma'ale Adumim	31.75	35.31
WB	HUJ 21643	---	*	---	---	---	---	Israel, Gilbo'a: Ma'ale Merav	32.44	35.44
WB	HUJ 21929	---	*	---	---	---	---	Unknown location	---	---
WB	HUJ 22161	---	*	---	---	---	---	Unknown location	---	---
WB	HUJ 3652	---	*	---	---	---	---	Israel, Bab el Wad	31.81	35.02
WB	HUJ 8431	---	*	---	---	---	---	Israel, Dead Sea: NAhal Darga	31.57	35.39
WB	HUJ 8546	---	*	---	---	---	---	Israel, Btw. Mizpe Shalem and Jerusalem, near The Dead Sea	31.64	35.35
WB	HUJ 8573	---	*	---	---	---	---	Israel, 3 km W Ma'ale Adumim	31.77	35.3
WB	HUJ 8697	---	*	---	---	---	---	Israel, Jerusalem - Jericho road, 16 km from Jericho	---	---
WB	HUJ 8700	---	*	---	---	---	---	Israel, 'En Gedi	31.45	35.38
WB	HUJ 8727	---	*	---	---	---	---	Israel, 'En Gedi	31.45	35.38
WB	HUJ 8948	---	*	---	---	---	---	Israel, Ma'ale Efrayim-Pazael jnct., 200m towards former	32.06	35.42

……continued on the next page

APPENDIX 1. (Continued)

Species / Morph	Voucher	Genbank accession	Morphology	Genetic sample #	*COI*	*12S*	*cytb*	Location	Latitude	Longitude
WB	HUJ 8970	---	*	---	---	---	---	Israel, Hirbet Bani Fadil	32.08	35.37
WB	SMNH 10228	---	*	---	---	---	---	Israel, Wadi Balat	31.51	34.62
WB	SMNH 11230	---	*	---	---	---	---	Israel, Karmel	32.84	34.98
WB	SMNH 12638	---	*	---	---	---	---	Israel, Har Arbel	32.82	35.5
WB	SMNH 13098	---	*	---	---	---	---	Israel, Sasa	33.03	35.4
WB	SMNH 13673	---	*	---	---	---	---	Israel, Nebi Mussa	31.78	35.43
WB	SMNH 13674	---	*	---	---	---	---	Israel, Yericho	31.86	35.45
WB	SMNH 13675	---	*	---	---	---	---	Israel, Yericho	31.86	35.45
WB	SMNH 13710	---	*	---	---	---	---	Israel, Nebi Mussa	31.78	35.43
WB	SMNH 15998	---	*	---	---	---	---	Israel, Near Hirbet Hureqanya	31.71	35.37
WB	SMNH 3581	---	*	---	---	---	---	Israel, Nahal Ze'elim	31.25	35.2
WB	SMNH 7059	---	*	---	---	---	---	Israel, Yaa'r HaQdoshim	31.77	35.03
WB	SMNH 9295	---	*	---	---	---	---	Israel, Tubas (Shchem)	32.32	35.37
WNB	SMNH 15923	MF767364, MF767305, MF767368	*	1	*	*	*	Israel, Road no. 40 near Mizpe Ramon	30.62	34.83
WNB	SMNH 16372	MF767307, MF767370	---	2	---	*	*	Israel, Israel	---	---
WNB	SMNH 15939	MF767356, MF767308, MF767371	*	3	*	*	*	Israel, Zomet Zipporim south	30.83	34.75
WNB	SMNH 15924	MF767362, MF767309, MF767372	*	4	---	*	*	Israel, Mizpe Ramon	30.61	34.8
WNB	SMNH 15885	MF767310	---	5	---	*	---	Israel, Israel (Hai Ramon)	---	---
WNB	SMNH 16190	MF767350, MF767311, MF767373	*	6	*	*	*	Israel, Nahal Arugot	31.46	35.39
WNB	SMNH 16624	MF767351, MF767313, MF767375	*	8	*	*	*	Israel, Yotvata north. Road no. 90	29.92	35.06
WNB	SMNH 15306	MF767314, MF767376	*	9	---	*	*	Israel, Israel (Hai Ramon)	---	---
WNB	SMNH 16803	MF767315, MF767377	*	10	---	*	*	Israel, Ramon Air force base (access road)	30.77	34.67

……continued on the next page

APPENDIX 1. (Continued)

Species / Morph	Voucher	Genbank accession	Morphology	Genetic sample #	*COI*	*12S*	*cytb*	Location	Latitude	Longitude
WNB	SMNH 16664	MF767366, MF767316, MF767378	*	11	*	*	*	Israel, Hazeva	30.62	35.19
WNB	SMNH 15922	MF767354, MF767317, MF767379	*	12	*	*	*	Israel, Road no. 40 near Mizpe Ramon	30.62	34.83
WNB	SMNH 15794	MF767355, MF767318, MF767380	---	13	*	*	*	Israel, Mizpe Ramon	30.61	34.8
WNB	SMNH 17108	MF767358, MF767320, MF767382	*	15	*	*	*	Israel, Mizpe Ramon	30.61	34.81
WNB	SMNH 17242	MF767365, MF767323, MF767385	*	18	*	*	*	Israel, Dimona	31.06	35.03
WNB	HUJ 21718	MF767357, MF767325, MF767387	*	20	*	*	*	Israel, Yeruham	30.98	34.92
WNB	HUJ 21844	MF767352, MF767326	*	21	*	*	---	Israel, near Arad	31.25	35.21
WNB	SMNH 17410	MF767330, MF767390	*	25	---	*	*	Israel, Mizpe Ramon	30.61	34.8
WNB	HUJ 22279	MF767332	*	26	---	*	---	Israel, North Arava: road 90	30.68	35.22
WNB	HUJ 22280	MF767333, MF767392	*	27	---	*	*	Israel, Timna Be'er Ora: road 90	29.75	35.01
WNB	HUJ 22281	MF767334, MF767393	*	28	---	*	*	Israel, Be'er Ora	29.71	34.98
WNB	HUJ 22282	MF767335, MF767394	*	29	---	*	*	Israel, Elat: Williams House, road 90	29.52	34.92
WNB	HUJ 22283	MF767336, MF767395	*	30	---	*	*	Israel, Elat Mts: road 12	29.58	34.88
WNB	HUJ 22284	MF767337, MF767396	*	31	---	*	*	Israel, Qibbuz Elot	29.58	34.96
WNB	ZFMK 82627	MF767341	*	35	---	*	---	Egypt, Sinai, 2 km N turn-off Nabq	28.04	34.43
WNB	ZFMK 92820	MF767342, MF767400	*	36	---	*	*	Egypt, Sinai, Dahab Village	28.49	34.5
WNB	FMNH 153044 (PT)	---	*	---	---	---	---	Egypt, Helwan, Wadi Hof' [Hulwan, Wadi Hawfl]	29.87	31.32
WNB	FMNH 72108 (HT)	---	*	---	---	---	---	Egypt, St. Katarina Monestry area, Wadi el Sheikh	28.56	33.98

……continued on the next page

APPENDIX 1. (Continued)

Species / Morph	Voucher	Genbank accession	Morphology	Genetic sample #	*COI*	*12S*	*cytb*	Location	Latitude	Longitude
WNB	FMNH 72110 (HT)	---	*	---	---	---	---	Egypt, St. Katarina Monestry area, Wadi el Sheikh	28.56	33.98
WNB	HUJ 16617	---	*	---	---	---	---	Israel, Makhtesh Katan	30.96	35.19
WNB	HUJ 16849	---	*	---	---	---	---	Israel, Hazeva Field School	30.76	35.27
WNB	HUJ 16940	---	*	---	---	---	---	Israel, Hazeva Field School	30.76	35.27
WNB	HUJ 20803	---	*	---	---	---	---	Israel, Hazeva Field School	30.76	35.27
WNB	HUJ 20849	---	*	---	---	---	---	Israel, Hazeva Field School	30.76	35.27
WNB	HUJ 20855	---	*	---	---	---	---	Israel, Nahal 'Afran	30.91	34.91
WNB	HUJ 20893	---	*	---	---	---	---	Israel, 500m S of the Dead Sea Works gate (on highway)	31.02	35.36
WNB	HUJ 20927	---	*	---	---	---	---	Unknown location	---	---
WNB	HUJ 20940	---	*	---	---	---	---	Israel, Hazeva Field School	30.77	35.23
WNB	HUJ 20944	---	*	---	---	---	---	Israel, Arava: Moshav Hazeva (in fields)	30.77	35.28
WNB	HUJ 20997	---	*	---	---	---	---	Israel, Mizpe Ramon	30.61	34.8
WNB	HUJ 21037	---	*	---	---	---	---	Israel, Sede Boqer: Midrasha: International bldg.	30.84	34.77
WNB	HUJ 21048	---	*	---	---	---	---	Israel, 'En Gedi Nature Reserve: entrance to Nahal Dawid	31.46	35.38
WNB	HUJ 21049	---	*	---	---	---	---	Israel, 'En Gedi Nature Reserve: road to Nahal 'Arugot	31.46	35.38
WNB	HUJ 21123	---	*	---	---	---	---	Israel, on rd from Tlalim jnct to Halukim jnct, 3km from latter	30.89	34.77
WNB	HUJ 21572	---	*	---	---	---	---	Israel, circa 'En Gedi junction	31.45	35.38
WNB	HUJ 21720	---	*	---	---	---	---	Israel, near 'En 'Avdat	30.82	34.76
WNB	HUJ 21721	---	*	---	---	---	---	Israel, Mizpe Ramon: Ramon school	30.6	34.8
WNB	HUJ 21722	---	*	---	---	---	---	Israel, Mizpe Ramon: Alpaca farm	30.61	34.8
WNB	HUJ 21795	---	*	---	---	---	---	Israel, Negev	---	---
WNB	HUJ 21796	---	*	---	---	---	---	Israel, Negev	---	---
WNB	HUJ 21797	---	*	---	---	---	---	Israel, Negev	---	---
WNB	HUJ 21875	---	*	---	---	---	---	Israel, Biq'a road (road #90)	---	---
WNB	HUJ 21876	---	*	---	---	---	---	Israel, southern Judean desert: road #25, Zafit junction	31.04	35.2
WNB	HUJ 21877	---	*	---	---	---	---	Israel, southern Judean desert: Arad area	31.25	35.21
WNB	HUJ 21878	---	*	---	---	---	---	Israel, Wadi Yahel	31.18	35.23
WNB	HUJ 21879	---	*	---	---	---	---	Israel, Samar	29.83	35.02
WNB	HUJ 21880	---	*	---	---	---	---	Israel, Qetura	29.96	35.06

……continued on the next page

APPENDIX 1. (Continued)

Species / Morph	Voucher	Genbank accession	Morphology	Genetic sample #	*COI*	*12S*	*cytb*	Location	Latitude	Longitude
WNB	HUJ 21881	---	*	---	---	---	---	Israel, Hazeva	30.76	35.27
WNB	HUJ 21882	---	*	---	---	---	---	Israel, road #90, km 83	30.14	35.12
WNB	HUJ 22044	---	*	---	---	---	---	Israel, road #40	---	---
WNB	HUJ 22130	---	*	---	---	---	---	Israel, Moshav Idan	30.8	35.3
WNB	HUJ 22131	---	*	---	---	---	---	Israel, Qibbuz Samar	29.83	35.02
WNB	HUJ 22233	---	*	---	---	---	---	Israel, Negev: Yeruham Lake	30.98	34.9
WNB	HUJ 3184	---	*	---	---	---	---	Israel, S of Dead Sea	---	---
WNB	HUJ 3413	---	*	---	---	---	---	Israel, Sedom	31.06	35.39
WNB	HUJ 3590	---	*	---	---	---	---	Israel, 'En Gedi	31.45	35.38
WNB	HUJ 3631	---	*	---	---	---	---	Israel, Arava	---	---
WNB	HUJ 8322	---	*	---	---	---	---	Egypt, Qadesh Barne'a	30.9	34.4
WNB	HUJ 8326	---	*	---	---	---	---	Egypt, Branch of Wadi B'ab'a'a	28.95	33.25
WNB	HUJ 8340	---	*	---	---	---	---	Egypt, Wadi Ramkhan, S of St. Katarina Monestry	28.56	33.98
WNB	HUJ 8378	---	*	---	---	---	---	Egypt, Wadi Saghara, N slope of Jebel Habashi	28.63	34.16
WNB	HUJ 8392	---	*	---	---	---	---	Egypt, Gebel Musa, Bir Senobar	28.54	33.97
WNB	HUJ 8487	---	*	---	---	---	---	Egypt, Mitle camp	30.05	33.01
WNB	HUJ 8488	---	*	---	---	---	---	Egypt, Mitle camp	30.05	33.01
WNB	HUJ 8571	---	*	---	---	---	---	Egypt, Bir Sarir, btw, Nueiba and Dahav	28.84	34.57
WNB	HUJ 8590	---	*	---	---	---	---	Israel, 2 km N of 'En Gedi	31.45	35.38
WNB	HUJ 8691	---	*	---	---	---	---	Egypt, Zuqei David Field School	28.56	33.98
WNB	HUJ 8713	---	*	---	---	---	---	Egypt, Naqeb-el-Hu'e, 2 km from the Bussila	28.66	33.98
WNB	HUJ 8719	---	*	---	---	---	---	Egypt, Wadi Ihimer (Wadi Chilfieh)	28.2	34.11
WNB	HUJ 8720	---	*	---	---	---	---	Israel, 'En Yahav	30.65	35.23
WNB	HUJ 8768	---	*	---	---	---	---	Egypt, Thomelat Hawra	29.55	34.81
WNB	HUJ 8796	---	*	---	---	---	---	Egypt, nr. St. Katharina	28.55	33.97
WNB	HUJ 8798	---	*	---	---	---	---	Egypt, Zuqei David Field School	---	---
WNB	HUJ 8799	---	*	---	---	---	---	Egypt, Zuqei David Field School	---	---
WNB	HUJ 8851	---	*	---	---	---	---	Israel, Sede Boqer: within 5 km of Midrasha	30.85	34.78
WNB	HUJ 8877	---	*	---	---	---	---	Egypt, Sinai, in Zuqe Dawid Field School	28.56	33.98
WNB	HUJ 8950	---	*	---	---	---	---	Israel, Elat	29.55	34.94
WNB	HUJ 8951	---	*	---	---	---	---	Israel, Sede Boqer (Midrasha)	30.85	34.78

……continued on the next page

APPENDIX 1. (Continued)

Species / Morph	Voucher	Genbank accession	Morphology	Genetic sample #	*COI*	*12S*	*cytb*	Location	Latitude	Longitude
WNB	SMNH 10212	---	*	---	---	---	---	Egypt, Refidim	30.41	33.15
WNB	SMNH 11488 (PT)	---	*	---	---	---	---	Israel, Nahal Nekarot	30.53	34.74
WNB	SMNH 1324	---	*	---	---	---	---	Israel, Sede Boqer	30.87	34.79
WNB	SMNH 13251	---	*	---	---	---	---	Israel, Yotvata	29.89	35.05
WNB	SMNH 13843	---	*	---	---	---	---	Israel, Nahal Shelomo	29.58	34.89
WNB	SMNH 145	---	*	---	---	---	---	Israel, Har Horesha	30.56	34.52
WNB	SMNH 146	---	*	---	---	---	---	Israel, Be'er Yeroham	30.99	34.91
WNB	SMNH 147	---	*	---	---	---	---	Israel, Southern Negev	---	---
WNB	SMNH 15926	---	*	---	---	---	---	Israel, Mizpe Ramon	30.61	34.8
WNB	SMNH 16451	---	*	---	---	---	---	Israel, Ramat Matred	30.77	34.68
WNB	SMNH 1662 (PT)	---	*	---	---	---	---	Israel, 'En Yotvata	29.88	35.04
WNB	SMNH 2037	---	*	---	---	---	---	Israel, Yotvata	29.89	35.05
WNB	SMNH 2247	---	*	---	---	---	---	Israel, Sedom	31.07	35.39
WNB	SMNH 4430 (PT)	---	*	---	---	---	---	Israel, HaMakhtesh HaQatan	30.93	35.18
WNB	SMNH 8004 (PT)	---	*	---	---	---	---	Egypt, St. Katarina Monestry area	28.51	33.96
WNB	SMNH 8187 (PT)	---	*	---	---	---	---	Egypt, Vaset (Nueiba)	29.03	34.58
WNB	SMNH 854	---	*	---	---	---	---	Israel, Be'er Menuha	30.3	35.13
WNB	SMNH 9024	---	*	---	---	---	---	Israel, Eilot	29.57	34.96
WNB	SMNH 9427	---	*	---	---	---	---	Israel, Sede Boqer	30.87	34.79
WNB	SMNH 9603	---	*	---	---	---	---	Egypt, Jabel Yalak	30.38	33.51
P. collaris	MHNG 2447.75	AY039157	---	F06	---	*	---	Israel, Tel Aviv	---	---
P. collaris	MHNG 2447.74	AY039133	---	F07	---	*	---	Israel, Tel Aviv	---	---
P. collaris	HLMD J14	AY486922	---	F08	---	---	*	Jordan	---	---
P. karelini	MHNG 2443.3	AY647232	---	F17	---	*	---	Uzbekistan	---	---
P. karelini	CAS 184636	AY486918	---	F18	---	---	*	Turkmenistan	---	---
P. r. ladacensis	NMW 25452.1	---	*	---	---	---	---	India, Spiti Valley, junction of Parang and Spiti River, Sumdo area	---	---
P. r. rhodorachis	CAS 251164	MF767331, MF767391	---	F01	---	*	*	Oman, Wadi Bani Habib, 2.9 km (airline) WSW Sayq, Jebel Akhdar, Ad Dakhiliyah Region	23.07	57.6

……continued on the next page

APPENDIX 1. (Continued)

Species / Morph	Voucher	Genbank accession	Morphology	Genetic sample #	*COI*	*12S*	*cytb*	Location	Latitude	Longitude
P. r. rhodorachis	ZFMK 94291	MF767343	*	F02	---	---	---	Iran, Baluchistan, Nikh Shahr	---	
P. r. rhodorachis	CAS 185035	AY486921	---	F03	---	---	*	Turkmenistan, Ashkabad, 12 km NW Fyrusa	---	---
P. r. rhodorachis	BMNH 1869.8.28.127	---	*	---	---	---	---	Iran, Bushire [Bushehr City]	---	---
P. r. rhodorachis	BMNH 1874.11.25.11	---	*	---	---	---	---	Iran, south of Regan [Rigan]	---	---
P. r. rhodorachis	BMNH 1879.8.15.26	---	*	---	---	---	---	Iran, Shiraz [Shiraz City]	---	---
P. r. rhodorachis	BMNH 1886.9.21.100	---	*	---	---	---	---	Iran, Bezd [35.22, 60.43]	---	---
P. r. rhodorachis	BMNH 1919.7.18.12	---	*	---	---	---	---	Iran, Henjam Island [26.63, 55.87]	---	---
P. r. rhodorachis	BMNH 1936.10.12.6	---	*	---	---	---	---	Iran, Kerman [Kerman City]	---	---
P. r. rhodorachis	BMNH 1938.2.1.74	---	*	---	---	---	---	Saudi Arabia, Hadda, Wadi Fatuna, between Jidda and Mecca, S. Hejaz	---	---
P. r. rhodorachis	BMNH 1951.1.1.26	---	*	---	---	---	---	Iran, Masjed Soleyman, Khuzistan	---	---
P. r. rhodorachis	BMNH 1951.1.6.68	---	*	---	---	---	---	Iran, Jamal, Bariz	---	---
P. r. rhodorachis	BMNH 1979.708	---	*	---	---	---	---	Saudi Arabia, Sawawin	---	---
P. r. rhodorachis	BMNH 1985.802	---	*	---	---	---	---	Saudi Arabia, Taif	---	---
P. r. rhodorachis	CAS 135250	---	*	---	---	---	---	Saudi Arabia, Jiddah	---	---
P. r. rhodorachis	CAS 136479	---	*	---	---	---	---	Saudi Arabia, 80 km. NW & 2 km. W. of Mecca	---	---
P. r. rhodorachis	CAS 139528	---	*	---	---	---	---	Saudi Arabia, 112 km. S75 E of Taif	---	---
P. r. rhodorachis	CAS 140385	---	*	---	---	---	---	Saudi Arabia, Riyadh (Shamaysi)	24.63	46.71
P. r. rhodorachis	CAS 140498	---	*	---	---	---	---	Saudi Arabia, Jowa	17	43.1
P. r. rhodorachis	CAS 141076	---	*	---	---	---	---	Iran, Huvar [Sarbaz River]	26.15	61.45
P. r. rhodorachis	CAS 144208	---	*	---	---	---	---	Saudi Arabia, Abha	18.21	42.5
P. r. rhodorachis	CAS 148566	---	*	---	---	---	---	Saudi Arabia, 235 km Taif-Abha road	20	41.5

……continued on the next page

APPENDIX 1. (Continued)

Species / Morph	Voucher	Genbank accession	Morphology	Genetic sample #	*COI*	*12S*	*cytb*	Location	Latitude	Longitude
P. r. rhodorachis	CAS 148584	---	*	---	---	---	---	Saudi Arabia, Riyadh	24.63	49.63
P. r. rhodorachis	CAS 148615	---	*	---	---	---	---	Saudi Arabia, Jabal as Sinfa	27.95	35.78
P. r. rhodorachis	CAS 149437	---	*	---	---	---	---	Saudi Arabia, Wadi Jizan Dam	17.03	42.96
P. r. rhodorachis	CAS 149440	---	*	---	---	---	---	Saudi Arabia, between Abha and Al Qaraah	18.13	42.6
P. r. rhodorachis	CAS 157119	---	*	---	---	---	---	Iraq, Halabjah	35.16	45.98
P. r. rhodorachis	CAS 86371	---	*	---	---	---	---	Iran, between Masjed Soleyman and Haft Kel [Haftgel]	31.44	49.53
P. r. rhodorachis	CAS 86409	---	*	---	---	---	---	Iran, Masjed Soleyman	---	---
P. r. rhodorachis	CAS 86420	---	*	---	---	---	---	Iran, Masjed Soleyman	---	---
P. r. rhodorachis	CAS 86433	---	*	---	---	---	---	Iran, Naftak [Maidan-e Naftun]	31.96	49.25
P. r. rhodorachis	CAS 86586	---	*	---	---	---	---	Iran, Cham Kureh	31.51	49.83
P. r. rhodorachis	FMNH 141610	---	*	---	---	---	---	Iran, Iranshahr	27.2	60.7
P. r. rhodorachis	FMNH 141639	---	*	---	---	---	---	Iran, 5 km north of Pol-e Abgineh	29.55	51.77
P. r. rhodorachis	FMNH 171133	---	*	---	---	---	---	Iran, Mosharageh	31.02	49.43
P. r. rhodorachis	FMNH 171135	---	*	---	---	---	---	Iran, Jahrom	28.5	53.57
P. r. rhodorachis	FMNH 171136	---	*	---	---	---	---	Iran, 6 mi. NW Bastak	27.27	54.33
P. r. rhodorachis	FMNH 19618	---	*	---	---	---	---	Iraq, Diana [Diyana], near Rewandes [Rawandoz]	36.67	44.55
P. r. rhodorachis	FMNH 74615	---	*	---	---	---	---	Iraq, Sulimaniyah Liwa, entrance to Palegawra Cave	35.63	45.03
P. r. rhodorachis	MNHN 1961.134	---	*	---	---	---	---	Iran, Akinlou [Akanlu, Akenlu]	35.61	48.18
P. r. rhodorachis	MVZ 243947	---	*	---	---	---	---	Iran, Kerman Province, Dashtab, near Aliabad, along Rud Hane-ye Zar Dast	---	---
P. r. rhodorachis	NMW 18213.1	---	*	---	---	---	---	Afghanistan, 25 km north of Barikut [Bhirkot, Bar Kowt], [S Nuristan]	35.52	71.53
P. r. rhodorachis	NMW 34990.1	---	*	---	---	---	---	Iran, Shiraz	---	---

……continued on the next page

APPENDIX 1. (Continued)

Species / Morph	Voucher	Genbank accession	Morphology	Genetic sample #	*COI*	*12S*	*cytb*	Location	Latitude	Longitude
P. r. rhodorachis	NMW 34991.1	---	*	---	---	---	---	Iran, Shiraz	---	---
P. r. rhodorachis	NMW 34991.2	---	*	---	---	---	---	Iran, Darab	28.75	54.55
P. r. rhodorachis	ZFMK 31603	---	*	---	---	---	---	Iran, Fars, Shiraz area	---	---
P. r. rhodorachis	ZFMK 87118	---	*	---	---	---	---	Saudi Arabia, Thumama (national park), King Khalid Wildlife Center	25.27	46.55
P. r. rhodorachis	ZFMK 87119	---	*	---	---	---	---	Saudi Arabia, Wadi Hauta	---	---
P. r. rhodorachis	ZFMK 87243	---	*	---	---	---	---	Saudi Arabia, Taif	---	---
P. r. rhodorachis	ZFMK 94290	---	*	---	---	---	---	Iran, Bushehr, Khaeiz	---	---
P. rogersi	SMNH 16904	MG566073, MF767306, MF767369	---	F04	*	*	*	Israel, Central Negev	---	---
P. rogersi	NMW KCR2	AY188041	---	F05	---	---	*	Egypt, Sinai	---	---
Spalerosophis diadema	CAS 220641	AF471049	---	F09	---	---	*	Egypt	---	---
Spalerosophis diadema	HLMD J62	AY486926	---	F10	---	---	*	Jordan, Wadi Ram	---	---
Spalerosophis diadema	MHNG 2414.68	AY039148	---	F11	---	*	---	Pakistan	---	---
Hemorrhois nummifer	SH 548	AY039163	---	F15	---	*	---	Turkmenistan	---	---
Hemorrhois nummifer	ZISP 27709	AY376742	---	F16	---	---	*	Armenia	---	---
Spalerosophis diadema	MHNG 2547.44	AY039144	---	F12	---	*	---	Yemen, al-Hudaydah-Jizan, à 10 Km avant az-Zaydiyah, (Maro-fiyah)	---	---
Spalerosophis diadema	ROM 22879	KX694605.1, KX694865.1	---	F13 , F14	---	*	*	Unknown provenance (captive bred in Canada, Ontario)	---	---

APPENDIX 2. Results of a Student's t-test analyses (α = 0.05) between the left and right sides of the western sample specimens.

Character	Left		Right		P	Mean of the differences
	Mean	SD	Mean	SD		
DNE	3.15	0.80	3.34	0.84	<0.001	0.19
LW	1.38	0.39	1.39	0.39	0.155	0.02
LH	0.84	0.25	0.82	0.25	0.416	-0.01
CSU	4.11	1.03	4.17	1.04	0.003	0.06
CSL	5.06	1.32	4.99	1.26	0.203	-0.05
ED	3.01	0.58	3.05	0.59	0.004	0.05

APPENDIX 3. PCR primers and conditions used in this study.

Gene fragment	Primer	Sequence	Paper	PCR Parameters
cytb	L14910	5'-GACCTGTGATMTGAAAACCAYCGTTGT-3'	Burbrink *et al*., 2000	94°C 2', [94°C 40", 46°C 30", 72°C 1'] X35, 72°C 10', 10°C pause
	H16064	5'-CTTTGGTTTACAAGAACAATGCTTTA-3'		
12S	12S268(+)	5'-GTGCCAGCGACCGCGGTTACACG-3'	Schätti & Utiger, 2001	94°C 2', [94°C 1', 65°C 1', 72°C 1'] X35, 72°C 10', 10°C pause
	12S916(-)	5'-GTACGCTTACCATGTTACGACTTGCCCTG-3'		
COI	COI(+)degl	5'-AAGCTTCTGACTNCTACCACCNGC-3'	Schätti & Utiger, 2001	94°C 2', [94°C 1', 65°C 1', 72°C 1'] X35, 72°C 10', 10°C pause
	COI(-)bdeg	5'-ATTATTGTTGCYGCTGTRAARTAGGCTCG-3'		

APPENDIX 4. Comparison of value ranges of all of the continuous characters, between the western and the eastern samples. Results originating from the left side of a specimen are marked by an asterisk.

Character	Western sample				Eastern sample			
	Range	Mean	SD	n	Range	Mean	SD	n
SVL	210–1043	564.19	185.38	147	205–889	546.73	211.32	37
TL	74–365	211.69	70.31	88	80–326	194.12	79.97	25
TOL	284–1280	727.25	238.76	87	292–1204	688.92	274.17	25
TL/SVL	0.27–0.46	0.41	0.03	87	0.22–0.5	0.39	0.05	25
VENTRALS	217–264	237.16	11.66	127	206–254	228.18	10.27	33
SUBCAUDALS	113–158	135.10	7.84	81	114–189	134.28	13.37	25
SOMITES	334–420	370.35	17.46	71	340–384	358.75	14.05	20
DSRVL1917ex	120–151.5	136.35	6.60	79	112–145.5	128.85	8.11	23
DSRVL1715ex	128.5–156	140.85	6.24	79	120.5–146	134.15	7.24	23
DSRVL1513ex	146.5–201	167.92	12.58	78	130–212.5	155.69	17.52	21
DSRVL1917pct	51.78–61.89	57.21	2.46	79	52.11–60.63	56.52	1.99	21
DSRVL1715pct	53.91–63.3	59.09	2.15	79	55.2–61.3	58.96	1.67	21
DSRVL1513pct	62.02–88.16	70.50	6.01	78	62.5–88.54	68.46	6.05	20
DSRDL1918	2.5–9.5	5.73	2.10	83	2.5–8.5	7.07	1.62	28
DSRDL1817	2.5–9.5	5.52	2.12	83	1.5–9.5	6.89	1.99	28
DSRDL1716	1.5–9.5	5.27	2.02	83	3.5–7.5	4.57	1.36	28
DSRDL1615	1.5–9.5	5.05	2.09	83	2.5–8.5	4.54	1.45	28

.....continued on the next page

APPENDIX 4. (Continued)

Character	Western sample				Eastern sample			
	Range	Mean	SD	n	Range	Mean	SD	n
DSRDL1514	4.5–7.5	6.21	0.58	82	5.5–7.5	6.50	0.28	26
DSRDL1413	4.5–7.5	6.20	0.56	82	5.5–7.5	6.42	0.39	26
HL	9–20.7	14.14	2.83	148	6.7–24.4	14.84	4.18	41
HW	3.4–9.1	6.06	1.42	146	3.6–11.1	6.25	1.93	40
HL/HW	1.48–3.66	2.36	0.22	145	1.56–2.78	2.38	0.20	40
RW	1.3–4.9	2.90	0.75	145	1.8–5.7	3.24	1.10	38
RH	1.1–3.4	2.04	0.54	142	1.2–4.3	2.32	0.85	38
RW/RH	1.05–2	1.43	0.16	142	1.24-1.58	1.41	0.08	38
LW	0.4–2.4	1.39	0.40	139	0.6–2.7	1.50	0.55	41
LH	0.3–1.5	0.81	0.25	140	0.4–1.9	1.01	0.39	41
LW/LH	0.8–2.86	1.74	0.32	139	1–2.22	1.51	0.28	41
FL	3.1–7	4.88	0.86	149	3.2–7.7	5.01	1.19	41
FW	1.8–6.2	3.54	0.87	149	1.9–5.4	3.59	1.05	41
FL/FW	1.03–1.72	1.40	0.13	149	1.2–1.79	1.43	0.15	41
INP	1.4–6.1	3.51	0.97	147	1.4–6.1	3.55	1.20	41
FL/INP	0.97–2.21	1.43	0.19	147	1.16–2.43	1.48	0.25	41
PL	3.7–7.8	5.32	0.94	149	3.5–8.4	5.45	1.27	41
FL/PL	0.74–1.13	0.92	0.08	149	0.78–1.33	0.92	0.11	41
DNE	1.6–5.5	3.34	0.84	137	1.9–6.6	3.50	1.30	37
DNE*	1.5–5.2*	3.15*	0.8*	137*	1.7–6*	3.38*	1.15*	37*
DNE:INP	0.76–1.28	0.96	0.10	136	0.75–1.43	1.01	0.12	37
DNE:INP*	0.67–1.33*	0.9*	0.11*	136*	0.73–1.43*	0.98*	0.13*	37*
CSU	2.3–6.9	4.17	1.04	135	2.6–7.6	4.43	1.37	39
CSU*	2.2–7*	4.11*	1.03*	133*	2.4–8.1*	4.45*	1.47*	37*
CSL	3–8.4	5.01	1.27	135	3.2–10.3	5.81	1.88	39
CSU/CSL	0.62–1.08	0.83	0.09	133	0.65–0.98	0.77	0.08	38
CSU/CSL*	0.6–1.06*	0.82*	0.09*	132*	0.66–0.95*	0.77*	0.07*	36*
ED	1.8–4.3	3.05	0.59	121	1.8–4.8	3.08	0.83	34
ED*	1.8–4.2*	3.01*	0.58*	119*	1.6–4.7*	3.09*	0.84*	35*

APPENDIX 5. Frequency comparisons of categorical character states between the banded and the western and the eastern samples. P-values are for Fisher's exact tests. Results originating from the left side of a specimen are marked by an asterisk.

Character	P	States	Eastern	Western
DSRPOST	0.556	11	26	4
		13	103	31
		15	9	2
DSR4th	0.329	No	112	33
		Yes	26	4
TEMP	<0.001	2	122	13
		3	19	30
TEMP*	<0.001*	1*	3*	0*
		2*	105*	14*
		3*	31*	33*
SUPLA	0.411	8	1	1
		9	126	37
		10	7	1
SUPLA*	0.232*	8*	0*	1*
		9*	121*	37*
		10*	11*	2*
SUBLA	0.433	9	5	0
		10	106	36
		11	2	1
SUBLA*	0.308*	9*	4*	0*
		10*	108*	37*
		11*	1*	1*
PREOC	0.003	1	114	43
		2	21	0
PREOC*	0.007*	1*	118*	47*
		2*	17*	0*
POSTOC	1	1	2	0
		2	136	43
GUL	0.009	2	0	1
		3	36	3
		4	92	35
		5	5	2
GUL*	<0.001*	2*	0*	1*
		3*	25*	1*
		4*	99*	31*
		5*	7*	8*

APPENDIX 6. Comparison between character values of the type specimens of *Platyceps saharicus*, *P. r.* var. *tessellata*, *P. r. ladacensis* and *P. r. rhodorachis* and those of the banded and the non-banded color morphs of the western sample. B: banded. N.B: non-banded. Y: match, N: mismatch. Mismatches are bolded. Type specimens values are from Schätti & McCarthy (2004), Schätti *et al.* (2014) and from photographs courtesy of Tom Geerinckx (IRSNB).

Character	B.	N.B.	*P. saharicus* (FMNH 72108)	B.	N.B.	*P. r.* var. *tessellata* (IRSNB 2027)	B.	N.B.	*P. r. ladacensis* (ZSI 7323)	B.	N.B.	*P. r. rhodorachis* (MSNG 30312)	B.	N.B.
VENTRALS	217–238	218–264	250	**N**	Y	243	**N**	Y	237	Y	Y	227	Y	Y
SUBCAUDALS	113–141	124–158	144	**N**	Y	141 (incomplete)	**N**	NA	102 (missings)	NA	NA	142	**N**	Y
SOM	334–375	343–420	394	**N**	Y	At least 384	**N**	NA	At least 339	NA	NA	369	Y	Y
DSRANT	19	19	19	Y	Y	19	Y	Y	19	Y	Y	19	Y	Y
DSRMID	19	19	19	Y	Y	19	Y	Y	NA	NA	NA	NA	NA	NA
DSRPOST	11, 13, 15	11, 13, 15	11	Y	Y	12	**N**	**N**	NA	NA	NA	NA	NA	NA
DSRVL1917ex	124–145.5	120–151.5	134+135	Y	Y	142	Y	Y	NA	NA	NA	NA	NA	NA
DSRVL1715ex	129.5–148	128.5–156	142	Y	Y	142	Y	Y	NA	NA	NA	NA	NA	NA
DSRVL1513ex	153.5–201	146.5–199	157+158	Y	Y	159-160	Y	Y	NA	NA	NA	NA	NA	NA
DSRVL1917pct	54–62	52–61	54	Y	Y	58.43	Y	Y	NA	NA	NA	NA	NA	NA
DSRVL1715pct	57–63	54–62	57	Y	Y	58.43	Y	Y	NA	NA	NA	NA	NA	NA
DSRVL1513pct	70–88	62–81	63	**N**	Y	65.84	Y	Y	NA	NA	NA	NA	NA	NA
DSRDL1918	2.5–9.5	2.5–9.5	6.5	Y	Y	2.5	Y	Y	NA	NA	NA	NA	NA	NA
DSRDL1817	3.5–8.5	2.5–9.5	7.5	Y	Y	2.5	**N**	Y	NA	NA	NA	NA	NA	NA
DSRDL1716	1.5–9.5	2.5–8.5	3.5	Y	Y	7 (=6.5 or 7.5)	Y	Y	NA	NA	NA	NA	NA	NA
DSRDL1615	1.5–8.5	1.5–9.5	3.5	Y	Y	7 (=6.5 or 7.5)	Y	Y	NA	NA	NA	NA	NA	NA
DSRDL1514	5.5–7.5	4.5–7.5	6.5	Y	Y	6.5	Y	Y	NA	NA	NA	NA	NA	NA
DSRDL1413	5.5–7.5	4.5–7.5	6.5	Y	Y	6.5	Y	Y	NA	NA	NA	NA	NA	NA
DSR4th	Yes, No	Yes, No	Yes	Y	Y	Yes	Y	Y	NA	NA	NA	NA	NA	NA
SVL	234–804	210–1043	905	**N**	Y	523	Y	Y	NA	NA	NA	405	Y	Y
TL	84–310	74–365	365	**N**	Y	221 (stump)	NA	NA	NA	NA	NA	180	Y	Y
TOL	318–1114	284–1280	1270	**N**	Y	At least 744	NA	NA	NA	NA	NA	585	Y	Y
TL/SVL	0.36–0.45	0.27–0.46	0.4	Y	Y	NA	NA	NA	NA	NA	NA	0.44	Y	Y
AP	Divided	Divided	Divided	Y	Y	Divided	Y	Y	Divided	Y	Y	Divided	Y	Y

……continued on the next page

APPENDIX 6. (Continued)

Character	B.	N.B.	*P. saharicus* (FMNH 72108)	B.	N.B.	*P. r.* var. *tessellata* (IRSNB 2027)	B.	N.B.	*P. r. ladacensis* (ZSI 7323)	B.	N.B.	*P. r. rhodorachis* (MSNG 30312)	B.	N.B.
STE	2	2	2	Y	Y	2	Y	Y	2	Y	Y	2	Y	Y
TEMP	1, 2, 3	2, 3	2	Y	Y	3	Y	Y	2	Y	Y	1	Y	**N**
SUPLA	9, 10	8, 9, 10	9	Y	Y	9	Y	Y	9	Y	Y	9	Y	Y
SUBLA	9, 10	9, 10, 11	10	Y	Y	10	Y	Y	NA	NA	NA	10/9	Y	Y
PREOC	1, 2	1, 2	1	Y	Y	1	Y	Y	1	Y	Y	2	Y	Y
POSTOC	1, 2	2	2	Y	Y	2	Y	Y	2	Y	Y	2	Y	Y
SUBOCS	1	1	1	Y	Y	1	Y	Y	NA	NA	NA	NA	NA	NA
GUL	3, 4, 5	3, 4, 5	4	Y	Y	4	Y	Y	NA	NA	NA	NA	NA	NA
HL/HW	2.1–3.7	1.5–3.7	2.3	Y	Y	2.1	Y	Y	NA	NA	NA	NA	NA	NA
RW/RH	1.1–1.9	1.2–2	>1	Y	Y	1.4	Y	Y	1	**N**	**N**	NA	NA	NA
LH	1.2–2.4	0.8–2.9	>1	Y	Y	NA	NA	NA	~1	Y	Y	NA	NA	NA
FW	1.2–1.7	1–1.7	1.5	Y	Y	1.3	Y	Y	NA	NA	NA	NA	NA	NA
INP	1.2–1.8	1–2.2	1.5	Y	Y	1.6	Y	Y	NA	NA	NA	NA	NA	NA
PL	0.8–1	0.7–1.1	1	Y	Y	1.0	Y	Y	NA	NA	NA	NA	NA	NA
DNE	0.7–1	0.7–1.3	~1	Y	Y	1.0	Y	Y	NA	NA	NA	NA	NA	NA
CSL	0.7–1.1	0.6–1	<1	Y	Y	NA	NA	NA	NA	NA	NA	NA	NA	NA

APPENDIX 7. Sequence divergence (uncorrected *p-distances*) based on *12S* gene and *cytb* gene (in parenthesis) for all taxa compared.

Banded	0.4 (0.6)					
P. rogersi	3.1 (6.6)	3.4 (6.8)	3.2 (6.7)			
P. rhodorachis	5.9 (12)	5.7 (12)	5.8 (12)	6.4 (11.1)		
P. karelini	5.4 (11.6)	5.2 (11.7)	5.3 (11.6)	5.9 (12.4)	5.6 (13.7)	
P. collaris	7.6 (13.6)	7.5 (13.4)	7.5 (13.5)	8.5 (11.6)	8.4 (13.5)	7.3 (16.1)
	Non-banded	Banded	Western	P. rogersi	P. rhodorachis	P. karelini